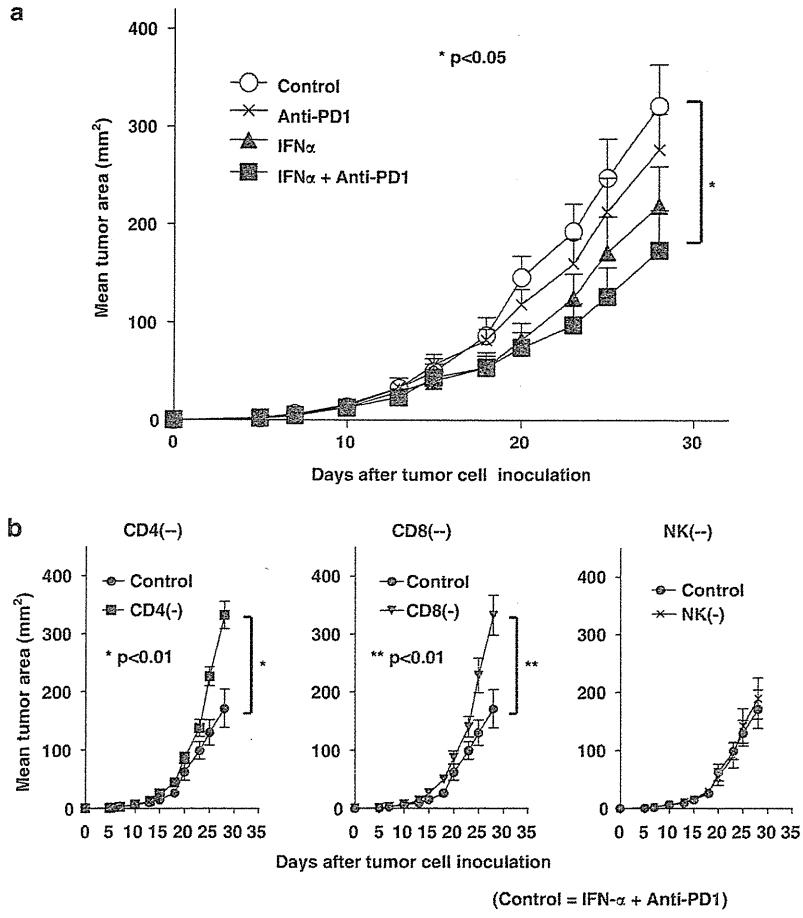

Figure 2. (**a**) Therapeutic inoculations with the combination of interferon (IFN)-α-transduced MC38 tumor cells and the anti-programmed cell death-1 (PD-1) antibody suppress the *in vivo* growth of established MC38 tumors. Animals were inoculated with MC38-wild type (WT) in the flank on day 0. Established MC38 cells were treated three times with MC38-IFNα alone, anti-PD-1 antibody alone or the combination in the contralateral flank every third day starting 7 days after WT tumor injection. (**b**) $CD4^+$ and $CD8^+$ cells are responsible for antitumor effects induced by combination of IFN-α and anti-PD-1. Mice were depleted of $CD4^+$ T cells, $CD8^+$ T cells or asialo-$GM1^+$ cells using specific antibodies 3 days before the WT tumor inoculation. MC38-IFNα and anti-PD-1 antibody combination therapy was performed every third day starting 7 days after WT tumor injection. Six mice were studied in each group. The results are reported as mean tumor area (mm^2) ± s.e. Significance at the 95% confidence limits is indicated. This experiment was performed twice with similar results.

Table 2. Immunohistologic analysis of $CD8^+$ T-cell infiltration in the established wild-type tumors treated with MC38-IFN-α and/or anti-PD-1 antagonistic antibody

Treatment	*Number of positive cells*			
	$CD4^+$ cells	*$CD8^+$cells*	*$CD11c^+$ cells*	*Gr-1^+ cells*
Control	3.6 ± 3.6	7.8 ± 6.1	3.3 ± 1.9	4.6 ± 9.0
Anti-PD-1	58.4 ± 55.4	33.8 ± 45.6	1.7 ± 1.8	0.8 ± 1.2
IFN-α	11.8 ± 6.4	15.0 ± 10.2	0.5 ± 1.2	0.8 ± 0.4
IFN-α+anti-PD-1	60.0 ± 44.8	33.2 ± 7.1	5.5 ± 5.8	2.5 ± 3.5

Abbreviations: IFN, interferon; PD-1, programmed cell death-1.
Immunoreactive cells were counted in five microscopic fields (400 ×) without knowledge of the experimental group. Results are reported as mean number of positive cells ± s.d.

did not see reductions in the size of all of the parental tumors. Therefore, further improvements in the treatment are needed before clinical application. In addition, we focused on PD-1, which has been identified as a marker of exhausted T cells.[16–22] As a blockade of PD-1 signaling has been shown to improve clinical outcome and restore functional T-cell responses in cancers,[32–34] we hypothesized that the PD-1 blockade had potential to enhance the Th1 responses elicited by the IFN-α gene-transduced tumor-based vaccination therapy. In this study, we investigated the antitumor effects and mechanisms of the combination of the IFN-α-transduced tumor cell vaccine therapy and PD-1 blockade.

First, we examined the *in vitro* effects of the IFN-α-transduced tumor cells and the anti-PD-1 antibody in a culture medium of splenocytes. Both IFN-α and the blockade of PD-1 obviously increased IFN-γ production and suppressed IL-10 production, and additive effects were observed with the combination of IFN-α and anti-PD-1. These results suggest that IFN-α and anti-PD-1 promoted Th1-type antitumor immune responses, and the responses were enhanced in cooperation with each other. From these results of the *in vitro* additive antitumor effects, we tried to treat tumor-bearing mice with the IFN-α and anti-PD-1 antibody, and a significant suppression of the outgrowth of the established tumors was observed only in the combination treatment group. The IFN-α or anti-PD-1 single therapy groups showed a weak, but not significant suppression of the established tumors compared with the control group. Leukocyte depletion

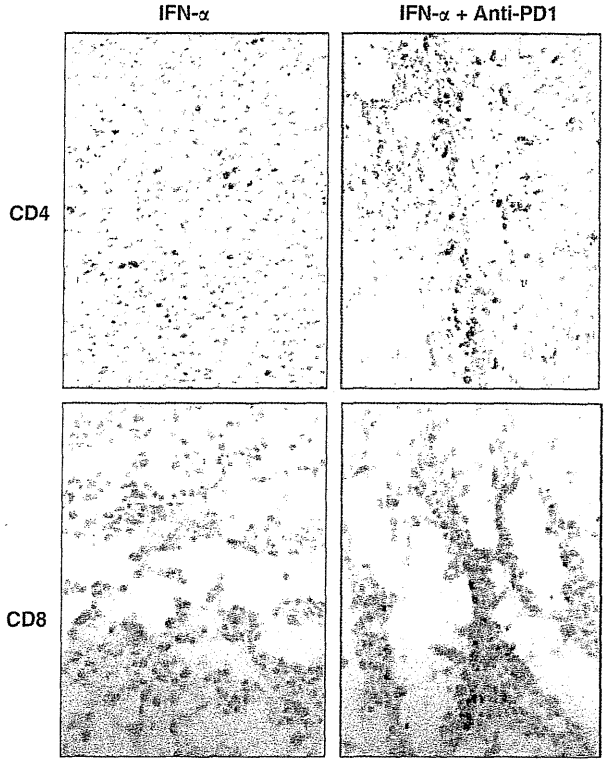

Figure 3. $CD4^+$ and $CD8^+$ cells markedly infiltrated into the established wild-type (WT) tumors of mice inoculated with the combination of MC38-interferon (IFN)-α cells and anti-programmed cell death-1 (PD-1) antibody. B6 mice were injected subcutaneously three times with MC38-IFNα cells and anti-PD-1-antibody either alone or in combination into the contralateral flank of the established WT tumor. Tumor tissues were harvested 4 days after therapeutic inoculation and stained with anti-CD4 and anti-CD8 antibodies. Immunoreactive cells were observed using light microscopy (400 ×).

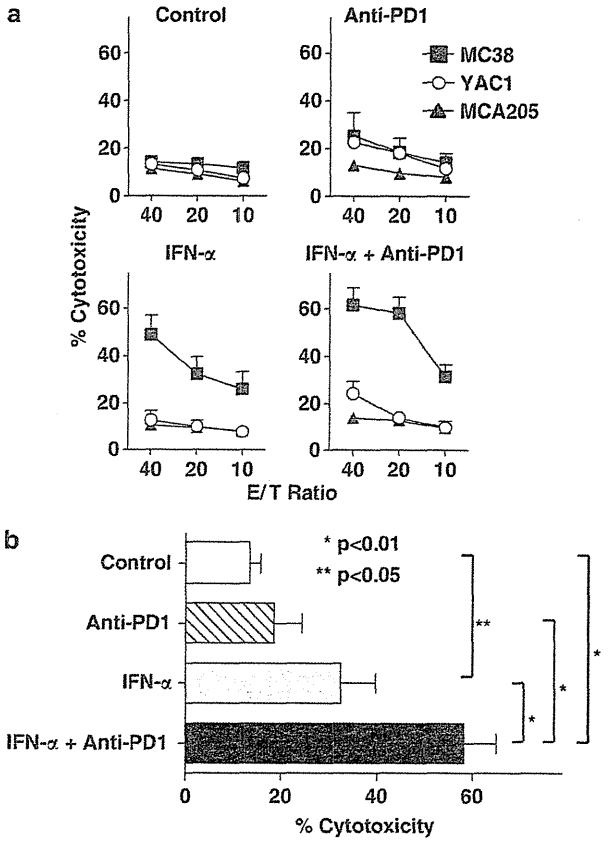

Figure 4. The combination treatment with interferon (IFN)-α and anti- programmed cell death-1 (PD-1) antibody induces potent tumor-specific cytolysis. (**a**) Mice were initially inoculated with MC38-IFNα cells and/or anti-PD-1 antibody on days 0, 7 and 14. Subsequently, MC38-immune mice received challenges of MC38-wild-type (WT) cells on day 28. Splenocytes were harvested from these mice on day 42 and then stimulated *in vitro* with MC38-IFNα cells and syngeneic dendritic cells twice weekly. The cytolytic assay against MC38, MCA205 or yeast artificial chromosome-1 (YAC-1) cells was performed 7 days after the last stimulation. Results are reported as mean percent cytotoxicity + s.d. This experiment was performed twice with similar results. (**b**) The cytolytic assay against MC38 was performed on an effector to target ratio of 20. E:T, effector to target.

experiments demonstrated that both $CD4^+$ T cells and $CD8^+$ T cells were essential to the tumor suppression induced by combination therapy. In contrast, the depletion of NK cell did not affect to the therapeutic effect in this model.

Immunohistologic analyses of the established tumors in the mice that were treated with anti-PD-1 showed marked infiltration of both $CD4^+$ cells and $CD8^+$ cells compared with controls and the group treated with MC38-IFNα alone. These data support the results of a previous study that showed that blockade of PD-1 signaling pathways reversed T-cell exhaustion and restored antitumor immunity.[34] Interestingly, the proliferation rate of splenocytes did not differ significantly between the control group and the anti-PD-1 treatment groups in the *in vitro* culture setting (data not shown). The conditions and microenvironment of the local tumor sites seemed to lead to this discrepancy between the *in vitro* and *in vivo* results because immunohistochemical staining confirmed that established MC38-WT tumors expressed abundant PD-L1 molecules (data not shown). However, we demonstrated that blockade of PD-1 reduced the level of apoptosis in lymphocytes on *in vitro* setting. These observations suggest that the PD-1 blockade prevented the apoptosis of lymphocytes and maintained the survival and infiltration of tumor-specific T cells in the local tumor environment, which strongly expressed PD-L1 molecules.

Although the PD-1 blockade recruited lymphocytes to the tumor sites, the therapeutic effects were not remarkable for the treatment with anti-PD-1 alone. In order to assess this result, we tried to induce tumor-specific CTLs from the splenocytes of IFN-α or anti-PD-1-treated mice and then perform cytolytic assays. A high specificity for MC38 was observed when treatment was performed with IFN-α, whereas only nonspecific cytolysis was detected with the anti-PD-1 treatment. Furthermore, specific cytolysis against MC38 was observed more potently with the combined IFN-α and anti-PD-1 treatment group compared with the IFN-α single treatment group. These observations suggest that IFN-α elicited tumor-specific CTLs, whereas the blockade of PD-1 mainly maintained the specific response induced by IFN-α, preventing CTLs from apoptosis. Thus, the combined therapy is considered to be reasonable because both IFN-α and the blockade of PD-1 revealed antitumor effects by different mechanisms. Also recent study show similar results and support our study that blockade of PD-1 can enhance the immune response stimulated by cytokine therapy in murine colon cancer model.[37]

The clinical use of this kind of tumor-based gene therapy may be limited because of the need to transduce genes in patients' tumor cells. IFN-α gene-transduced cells were used in this study, although the establishment of transduced cells, which produce a

high amount of IFN-α, would be difficult in the clinical setting. Administering recombinant IFN-α repetitively seems to be simple, but there was no therapeutic effect observed in our past study (data not published). In order to facilitate this, the method of cytokine gene delivery will need to be modified. In addition, it is not established whether anti-PD-1 therapy is effective against the tumors, which are negative for the expression of PD-L1. In order to resolve these problems, we are now planning to use other tumor cell lines and reevaluate the antitumor effects of the PD-1 blockade on the established tumors.

In conclusion, our findings suggest that the combination of IFN-α immunotherapy and PD-1 blockade therapy has potential for inducing potent immune responses and that this might be considered as a possible candidate for clinical trials of cancer vaccines, although further investigations are required.

CONFLICT OF INTEREST

The authors declare no conflict of interest.

ACKNOWLEDGEMENTS

We thank Ms Tomoe Shimazaki and Ms Hisako Nozawa for technical assistance. This study was supported in part by a Grant-in-Aid for Young Scientists (B) from the Ministry of Education, Culture, Sports, Science and Technology of Japan for JE; a Grant-in-Aid for Scientific Research (C) from the Ministry of Education, Culture, Sports, Science and Technology of Japan; and a grant from the Ministry of Health, Labor, and Welfare of Japan for KH.

REFERENCES

1 O'Connell J, Bennett MW, O'Sullivan GC, Collins JK, Shanahan F. The Fas counterattack: cancer as a site of immune privilege. *Immunol Today* 1999; **20**: 46–52.
2 Bronte V, Serafini P, Apolloni E, Zanovello P. Tumor-induced immune dysfunctions caused by myeloid suppressor cells. *J Immunother* 2001; **24**: 431–446.
3 Chen L, Linsley PS, Hellstrom KE. Costimulation of T cells for tumor immunity. *Immunol Today* 1993; **14**: 483–486.
4 Colombo MP, Forni G. Cytokine gene transfer in tumor inhibition and tumor therapy: where are we now? *Immunol Today* 1994; **15**: 48–51.
5 Musiani P, Modesti A, Giovarelli M, Cavallo F, Colombo MP, Lollini PL *et al.* Cytokines, tumour-cell death and immunogenicity: a question of choice. *Immunol Today* 1997; **18**: 32–36.
6 Eguchi J, Kuwashima N, Hatano M, Nishimura F, Dusak JE, Storkus WJ *et al.* IL-4-transfected tumor cell vaccines activate tumor-infiltrating dendritic cells and promote type-1 immunity. *J Immunol* 2005; **174**: 7194–7201.
7 Juang Y, Lowther W, Kellum M, Au WC, Lin R, Hiscott J *et al.* Primary activation of interferon A and interferon B gene transcription by interferon regulatory factor 3. *Proc Natl Acad Sci USA* 1998; **95**: 9837–9842.
8 Marie I, Durbin JE, Levy DE. Differential viral induction of distinct interferon-alpha genes by positive feedback through interferon regulatory factor-7. *EMBO J* 1998; **17**: 6660–6669.
9 Okada H, Villa L, Attanucci J, Erff M, Fellows WK, Lotze MT *et al.* Cytokine gene therapy of gliomas: effective induction of therapeutic immunity to intracranial tumors by peripheral immunization with interleukin-4 transduced glioma cells. *Gene Ther* 2001; **8**: 1157–1166.
10 Belardelli F. Role of interferons and other cytokines in the regulation of the immune response. *APMIS* 1995; **103**: 161–179.
11 von Hoegen P, Zawatzky R, Schirrmacher V. Modification of tumor cells by a low dose of Newcastle disease virus. III Potentiation of tumor-specific cytolytic T cell activity via induction of interferon-alpha/beta. *Cell Immunol* 1990; **126**: 80–90.
12 Hiroishi K, Tuting T, Lotze MT. IFN-alpha-expressing tumor cells enhance generation and promote survival of tumor-specific CTLs. *J Immunol* 2000; **164**: 567–572.
13 Eguchi J, Hiroishi K, Ishii S, Mitamura K. Interferon-alpha and interleukin-12 gene therapy of cancer; interferon-alpha induces tumor-specific immune responses while interleukin-12 stimulates non-specific killing. *Cancer Immunol Immunother* 2003; **52**: 378–386.
14 Eguchi J, Hiroishi K, Ishii S, Baba T, Matsumura T, Hiraide A *et al.* Interleukin-4 gene transduced tumor cells promote a potent tumor-specific Th1-type response in cooperation with interferon-alpha transduction. *Gene Ther* 2005; **12**: 733–741.
15 Ishida Y, Agata Y, Shibahara K, Honjo T. Induced expression of PD-1, a novel member of the immunoglobulin gene superfamily, upon programmed cell death. *EMBO J* 1992; **11**: 3887–3895.
16 Day CL, Kaufmann DE, Kiepiela P, Brown JA, Moodley ES, Reddy S *et al.* PD-1 expression on HIV-specific T cells is associated with T-cell exhaustion and disease progression. *Nature* 2006; **443**: 350–354.
17 Petrovas C, Casazza JP, Brenchley JM, Price DA, Gostick E, Adams WC *et al.* PD-1 is a regulator of virus-specific CD8+ T cell survival in HIV infection. *J Exp Med* 2006; **203**: 2281–2292.
18 Trautmann L, Janbazian L, Chomont N, Said EA, Gimmig S, Bessette B *et al.* Upregulation of PD-1 expression on HIV-specific CD8+ T cells leads to reversible immune dysfunction. *Nat Med* 2006; **12**: 1198–1202.
19 Urbani S, Amadei B, Tola D, Massari M, Schivazappa S, Missale G *et al.* PD-1 expression in acute hepatitis C virus (HCV) infection is associated with HCV-specific CD8 exhaustion. *J Virol* 2006; **80**: 11398–11403.
20 Penna A, Pilli M, Zerbini A, Orlandini A, Mezzadri S, Sacchelli L *et al.* Dysfunction and functional restoration of HCV-specific CD8 responses in chronic hepatitis C virus infection. *Hepatology* 2007; **45**: 588–601.
21 Boettler T, Panther E, Bengsch B, Nazarova N, Spangenberg HC, Blum HE *et al.* Expression of the interleukin-7 receptor alpha chain (CD127) on virus-specific CD8+ T cells identifies functionally and phenotypically defined memory T cells during acute resolving hepatitis B virus infection. *J Virol* 2006; **80**: 3532–3540.
22 Boni C, Fisicaro P, Valdatta C, Amadei B, Di Vincenzo P, Giuberti T *et al.* Characterization of hepatitis B virus (HBV)-specific T-cell dysfunction in chronic HBV infection. *J Virol* 2007; **81**: 4215–4225.
23 Blank C, Kuball J, Voelkl S, Wiendl H, Becker B, Walter B *et al.* Blockade of PD-L1 (B7-H1) augments human tumor-specific T cell responses *in vitro*. *Int J Cancer* 2006; **119**: 317–327.
24 Fourcade J, Kudela P, Sun Z, Shen H, Land SR, Lenzner D *et al.* PD-1 is a regulator of NY-ESO-1-specific CD8+ T cell expansion in melanoma patients. *J Immunol* 2009; **182**: 5240–5249.
25 Iwai Y, Ishida M, Tanaka Y, Okazaki T, Honjo T, Minato N. Involvement of PD-L1 on tumor cells in the escape from host immune system and tumor immunotherapy by PD-L1 blockade. *Proc Natl Acad Sci USA* 2002; **99**: 12293–12297.
26 Blank C, Brown I, Peterson AC, Spiotto M, Iwai Y, Honjo T *et al.* PD-L1/B7H-1 inhibits the effector phase of tumor rejection by T cell receptor (TCR) transgenic CD8+ T cells. *Cancer Res* 2004; **64**: 1140–1145.
27 Ahmadzadeh M, Johnson LA, Heemskerk B, Wunderlich JR, Dudley ME, White DE *et al.* Tumor antigen-specific CD8 T cells infiltrating the tumor express high levels of PD-1 and are functionally impaired. *Blood* 2009; **114**: 1537–1544.
28 Gehring AJ, Ho ZZ, Tan AT, Aung MO, Lee KH, Tan KC *et al.* Profile of tumor antigen-specific CD8 T cells in patients with hepatitis B virus-related hepatocellular carcinoma. *Gastroenterology* 2009; **137**: 682–690.
29 Dong H, Strome SE, Salomao DR, Tamura H, Hirano F, Flies DB *et al.* Tumor-associated B7-H1 promotes T-cell apoptosis: a potential mechanism of immune evasion. *Nat Med* 2002; **8**: 793–800.
30 Gao Q, Wang XY, Qiu SJ, Yamato I, Sho M, Nakajima Y *et al.* Overexpression of PD-L1 significantly associates with tumor aggressiveness and postoperative recurrence in human hepatocellular carcinoma. *Clin Cancer Res* 2009; **15**: 971–979.
31 Thompson RH, Dong H, Lohse CM, Leibovich BC, Blute ML, Cheville JC *et al.* PD-1 is expressed by tumor-infiltrating immune cells and is associated with poor outcome for patients with renal cell carcinoma. *Clin Cancer Res* 2007; **13**: 1757–1761.
32 Zhang L, Gajewski TF, Kline J. PD-1/PD-L1 interactions inhibit antitumor immune responses in a murine acute myeloid leukemia model. *Blood* 2009; **114**: 1545–1552.
33 Mumprecht S, Schurch C, Schwaller J, Solenthaler M, Ochsenbein AF. Programmed death 1 signaling on chronic myeloid leukemia-specific T cells results in T-cell exhaustion and disease progression. *Blood* 2009; **114**: 1528–1536.
34 Sakuishi K, Apetoh L, Sullivan JM, Blazar BR, Kuchroo VK, Anderson AC. Targeting Tim-3 and PD-1 pathways to reverse T cell exhaustion and restore anti-tumor immunity. *J Exp Med* 2010; **207**: 2187–2194.
35 Hiroishi K, Tuting T, Tahara H, Lotze MT. Interferon-alpha gene therapy in combination with CD80 transduction reduces tumorigenicity and growth of established tumor in poorly immunogenic tumor models. *Gene Ther* 1999; **6**: 1988–1994.
36 Ishii S, Hiroishi K, Eguchi J, Hiraide A, Imawari M. Dendritic cell therapy with interferon-alpha synergistically suppresses outgrowth of established tumors in a murine colorectal cancer model. *Gene Ther* 2006; **13**: 78–87.
37 Yu P, Steel JC, Zhang M, Morris JC, Waldmann TA. Simultaneous blockade of multiple immune system inhibitory checkpoints enhances antitumor activity mediated by interleukin-15 in a murine metastatic colon carcinoma model. *Clin Cancer Res* 2010; **16**: 6019–6028.

Interleukin-4 and CpG oligonucleotide therapy suppresses the outgrowth of tumors by activating tumor-specific Th1-type immune responses

ATSUSHI KAJIWARA*, HIROYOSHI DOI*, JUNICHI EGUCHI, SHIGEAKI ISHII, AYAKO HIRAIDE-SASAGAWA, MASASHI SAKAKI, RISA OMORI, KAZUMASA HIROISHI and MICHIO IMAWARI

Division of Gastroenterology, Department of Medicine, Showa University School of Medicine, Tokyo 142-8666, Japan

Received November 14, 2011; Accepted January 9, 2012

DOI: 10.3892/or.2012.1723

Abstract. Because IL-4 and CpG oligodeoxynucleotides (CpG-ODNs) are immune stimulants, we evaluated the antitumor effects of IL-4 gene therapy and CpG-ODN treatment in a poorly immunogenic murine cancer model. We used a murine colorectal cancer MC38 cell line overexpressing the IL-4 gene (MC38-IL4). Incubation with MC38-IL4 and CpG-ODN enhanced bone marrow-derived dendritic cell (DC) maturation *in vitro*. In addition, interferon (IFN)-γ production was significantly increased in naïve splenocytes after they were coincubated with MC38-IL4 and CpG-ODN. When mice bearing MC38 wild-type tumors were inoculated subcutaneously with MC38-IL4 cells and CpG-ODN, the outgrowth of established parental tumors was significantly suppressed compared to those in the MC38-IL4-treated group (IL-4 vs. IL-4 + CpG-ODN, P=0.015). A marked infiltration of $CD8^+$ cells in the established parental tumors of mice treated with MC38-IL4 and CpG-ODN was confirmed by immunohistochemical analyses (MC38-IL4, 2.8±1.9 cells/field vs. MC38-IL4 + CpG-ODN, 20.7±15.3 cells/field, P=0.027). Significant tumor-specific cytolysis was detected when splenocytes of MC38-IL4 + CpG-ODN-treated mice were stimulated by γ-irradiated MC38-IL4 cells and CpG-ODN twice weekly *in vitro* and used as effector cells in a chromium-release assay (32.2±3.5% for MC38 cells vs. 3.2±1.1% for YAC-1 cells; at an effector to target ratio of 40). These results suggest that IL-4 and CpG-ODN treatment promotes potent Th1-type antitumor immune responses. Therefore, the combination of IL-4 gene therapy and CpG-ODN treatment for cancer should be evaluated in clinical trials.

Correspondence to: Dr Kazumasa Hiroishi, Division of Gastroenterology, Department of Medicine, Showa University School of Medicine, 1-5-8 Hatanodai, Shinagawa-ku, Tokyo 142-8666, Japan
E-mail: hiroishi@med.showa-u.ac.jp

*Contributed equally

Key words: interleukin-4, CpG, Th1, cytotoxic T lymphocyte, colorectal cancer

Introduction

Several original treatments of cancer have been developed in the last decade. Many anticancer drugs, including molecule-targeted drugs, have been applied clinically. Although some of these drugs have dramatically changed the prognoses of a number of diseases, several harmful side effects were observed. Because cancer immunotherapy is thought to induce few adverse events compared to other therapies, such as chemotherapy and radiation, the establishment of novel treatments that elicit potent immune responses against cancer has been anticipated. Indeed, many clinical trials of such treatments have been conducted. However, most of them have shown only minimal effects, and immunotherapy has not yet been applied as a conventional clinical treatment for cancer. Moreover, patients with advanced cancer exhibit impaired immune responses. Therefore, new strategies are needed to induce more potent antitumor immunities.

We have previously reported the antitumor effects and mechanisms of cell-based immunotherapies that were combined with treatments with cytokines, such as interferon (IFN)-α (1-3), IL-4 (4) and IL-12 (1). The administration of each cytokine gene-transduced tumor cells appears to induce potent cellular immune responses. However, the antitumor immune response mechanisms that were induced by these cytokine therapies differ from each other. In particular, we reported that IL-4 treatment resulted in unique and interesting biological effects.

IL-4, which is a type-2 response inducer (5,6), plays a major role in both B-cell and T-cell development in the immune system (7). In addition, it causes a class switch of B cells, upregulates MHC class II and adhesion molecules, and prevents the apoptosis of T cells (8). With respect to the antitumor effects, IL-4 has a direct inhibitory effect on tumor cell growth *in vivo* and *in vitro* (9,10) and an antiangiogenic effect (11). It has been reported that IL-4 activates endothelia in the tumor microenvironment, which results in an increased infiltration of immune cells (12). Other reports have suggested

that eosinophils and neutrophils are responsible for the antitumor effects induced by IL-4 (13-15). In addition, a recent study demonstrated that local IL-4 delivery at the site of vaccination activates local dendritic cells (DCs), which play a critical role in the initiation, promotion, and regulation of host immune responses and promote type-1 T-helper (Th1) cell responses (16). In that investigation, IL-4 appeared to support DC maturation and enhance IL-12p70 secretion from DCs. Because these findings support the therapeutic effects of IL-4 on tumors, IL-4 has been applied in the clinical treatment of tumors (17,18).

The potent immunomodulator CpG is present at the expected frequency of about 1 in 16 bases in bacterial DNA, but it is hardly observed in vertebrate DNA. It has been reported that DNA vaccines and synthetic oligodeoxynucleotides (ODN) containing an unmethylated CpG motif promote Th1-type immune responses. CpG stimulates DCs through the toll-like receptor 9 and enhances DC maturation, which may improve therapeutic effects on established tumors. Recently, we reported the synergistic effects of the combination of CpG-ODN and IFN-α on DC maturation (19). Furthermore, DC-based therapy with CpG-ODN and IFN-α exhibited potent antitumor effects by inducing tumor-specific cytotoxic T-lymphocyte (CTL) responses (3).

Although we have previously demonstrated that IL-4 promotes a Th1-type antitumor immune response, evidence of the induction of a more potent immune response that diminishes established tumors *in vivo* is required before justification of a clinical trial. In the present study, we anticipated that the combination of IL-4 gene therapy and CpG-ODN would have additive effects on tumors. Thus, we investigated the antitumor effects of the combination therapy and the underlying mechanisms of these effects in order to determine whether the combined therapy would be appropriated in a clinical trial.

Materials and methods

Mice. Female C57BL/6 (B6) mice that were 6-8 weeks old were purchased from Sankyo Lab Service (Tokyo, Japan) for use in experiments when they were 8-12 weeks old. Mice were maintained in an animal care facility at Showa University. This study was approved by the Ethics Committee for Animal Experiments of Showa University (permission #2011-1111).

Cell lines, culture medium and reagents. The MC38 murine colorectal adenocarcinoma cell line (B6 mouse origin) and the YAC-1 lymphoma cell line were maintained in RPMI-1640 medium that was supplemented with 10% heat-inactivated fetal calf serum, 2 mM L-glutamine, 100 IU/ml penicillin, and 100 μg/ml streptomycin (complete medium; CM) in a humidified incubator with 5% CO_2 in air at 37°C. All cell culture reagents were purchased from Life Technologies Corp. (Gaithersburg, MD). CpG-ODN-1826 and non-CpG-ODN-1911 (used as control ODN) were synthesized by Sigma-Aldrich Japan (Tokyo, Japan). We confirmed that non-CpG-ODN-1911 did not affect DC maturation or have antitumor activity (19).

Genetically modified tumor cell lines. The MC38 tumor cells that were transduced using retroviral vectors according to standard protocols, as previously described (20), were selected for antibiotic resistance in CM containing 0.5 mg/ml G418 (Sigma-Aldrich Corp., St. Louis, MO). We have established a IL-4-overexpressing MC38 cell line (MC38-IL4), which produces a large amount of IL-4 (359.9±108.2 ng/10^6 cells/48 h) (4). A neomycin-resistant gene-transduced MC38 (MC38-Neo) cell line was used as a control (21). The growth rate of the MC38-IL4 cells did not differ from those of MC38-wild-type (WT) or MC38-Neo cells *in vitro*.

Phenotypic changes of DCs after coincubation with IL-4-overexpressing tumor cells and CpG-ODN. In order to observe the immunogenic effects of IL-4 and CpG-ODN on DC maturation, flow cytometry was performed using FACSCalibur (Nippon Becton-Dickinson Co., Ltd., Tokyo, Japan). Bone marrow-derived DCs were generated, as previously reported (2). We incubated the DCs ($5x10^6$-$6x10^6$ cells/flask) with either MC38-IL4 or MC38-Neo cells ($1x10^6$ cells) that were 100 Gy-irradiated in combination with 6 μg/ml of either CpG-ODN-1826 or non-CpG-ODN-1911 *in vitro*. After a 24-h incubation, cells were harvested and stained with fluorescein isothiocyanate (FITC)-conjugated monoclonal antibodies. The monoclonal antibodies used in this assay were FITC-conjugated anti-H-2Kb, I-Ab, CD80, and CD86 antibodies (obtained from Nippon Becton-Dickinson). The results were shown as ratios of the mean fluorescent intensity (MFI) of the DCs that were incubated with each monoclonal antibody to the MFI of DCs incubated with the FITC-conjugated control IgG antibody.

IFN-γ and IL-10 production in naïve splenocytes coinoculated with IL-4-overexpressing tumor cells and CpG-ODN in vitro. In order to assess the effects of IL-4 and CpG-ODN on immune balance, we performed an enzyme-linked immunosorbent assay (ELISA) of the representative Th1-type cytokine, IFN-γ and the representative Th2-type cytokine, IL-10. Splenocytes ($1x10^6$ cells/ml) from naive mice were stimulated with either MC38-IL4 or MC38-Neo cells ($1x10^5$ cells/ml) either alone or in combination with 6 μg/ml of CpG-ODN-1826 or non-CpG-ODN-1911 *in vitro*. After a 24-h incubation, we measured the concentrations of IFN-γ and IL-10 in the supernatant of each culture with ELISA using a commercially available kit, according to the manufacturer's instructions (mouse IFN-γ ELISA and mouse IL-10 ELISA, Thermo Fisher Scientific, Inc., Rockford, IL). This experiment was repeated twice.

Combination therapy of IL-4-overexpressing tumors with CpG-ODN in therapeutic models. In order to evaluate the *in vivo* therapeutic effects of the combination of IL-4-overexpressing tumor cells and CpG-ODN on established tumors, we measured the size of established MC38-WT tumors in mice before and after treatment, as previously described (21). In brief, B6 mice were first injected s.c. with $3x10^5$ MC38-WT cells in the right flank. Seven, 9, and 11 days after the WT inoculation, $3x10^5$ MC38-Neo or MC38-IL4 cells were inoculated s.c. with 30 μg/mouse of either CpG-ODN-1826 or non-CpG-ODN-1911 around the established parental tumors, which had reached 4-20 mm^2 in size. Otherwise, tumor-bearing B6 mice ($5x10^5$ MC38-WT cells/mouse) were inoculated $5x10^5$ MC38-Neo or MC38-IL4 cells were inoculated s.c. with either CpG-ODN-1826 or ODN-1911 in the same

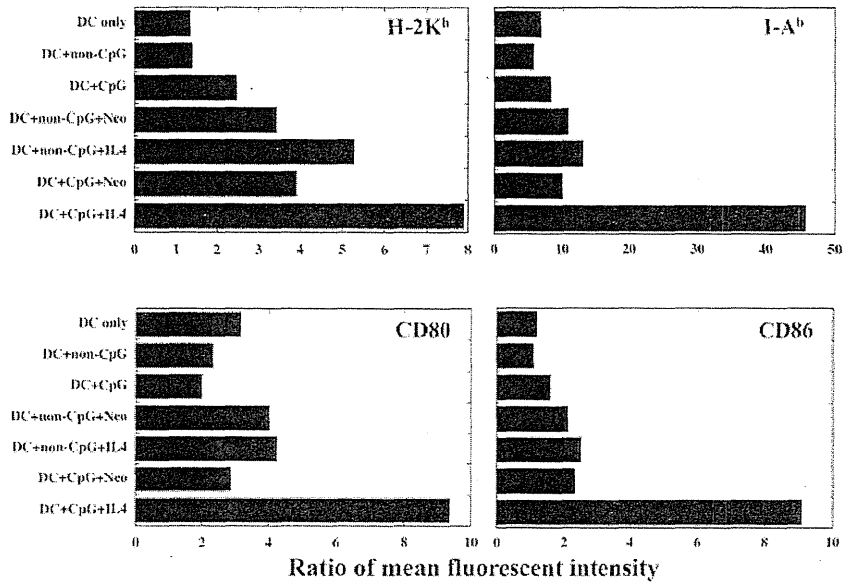

Figure 1. Coincubation with interleukin (IL)-4 and CpG-oligodeoxynucleotides (ODN) induces DC maturation *in vitro*. We incubated bone marrow-derived DCs with irradiated IL-4-overexpressing or control gene (Neo)-transduced MC38 cells either alone or in combination with CpG-ODN-1826 or non-CpG-ODN-1911 *in vitro*. Seven groups were compared: i) DC only, ii) DC + non-CpG, iii) DC + CpG, iv) DC + non-CpG + MC38-Neo, v) DC + non-CpG + MC38-IL4, vi) DC + CpG + MC38-Neo, and vii) DC + CpG + MC38-IL4. After a 24-h incubation, cells were stained with fluorescein isothiocyanate (FITC)-conjugated anti-H-2K^b, I-A^b, CD80, and CD86 monoclonal antibodies. The results are shown as ratios of mean fluorescent intensity (MFI) of the incubated DCs to the MFI of FITC-conjugated control IgG of each group.

manner. Tumor size was measured twice a week using vernier calipers. Each experiment involved 4-6 mice per group. Mice with ulcerated tumors or tumors >20 mm in diameter were sacrificed. Experiments with the therapeutic model were performed twice.

Immunohistological analysis. For leukocyte detection in tumor tissues, B6 mice were injected s.c. with $3x10^5$ MC38-Neo or -IL4 cells with or without 30 μg/mouse of CpG-ODN-1826 in the area surrounding the established wild-type tumor 7 days after inoculation with $3x10^5$ MC38-WT cells. Tumor tissues, which were harvested 3 days after inoculation with the genetically modified tumor. Serial 5-μm sections were exposed to anti-Gr-1, anti-CD11c, anti-CD4, and anti-CD8a antibodies (Nippon Becton-Dickinson). Rat IgG2a was used as a control antibody. Immunostaining was completed with a Vectastain ABC kit (Vector Laboratories, Inc., Burlingame, CA). Immunoreactive cells were counted in 6 fields in a light microscope (magnification, x400) in a blinded fashion.

Induction of tumor-specific CTL. We assessed the tumor-specific cytolytic activity of immune mice. Mice were initially immunized with MC38-IL4 cells in combination with 30 μg of either CpG-ODN-1826 or non-CpG-ODN-1911 on Day 0, and they were then inoculated with $3x10^5$ MC38-WT cells on Day 7. Subsequently, MC38-immune mice received a challenge of $1x10^6$ MC38-WT cells on Day 28. Splenocytes ($3x10^6$ cells/ml) were harvested from these mice on Day 42, and they were then stimulated in *vitro* with irradiated (100 Gy) MC38-IL4 tumor cells ($3x10^5$ cells/ml) and 6 μg/ml of non-CpG-ODN-1911 (IL-4 group) or IL4 cells in combination with 6 μg/ml of CpG-ODN-1826 (IL-4 + CpG group). Seven days later, responder cells ($1x10^6$ cells/ml) were restimulated with irradiated-IL4 tumor cells either alone (IL-4 group) or in combination with 6 μg/ml of CpG-ODN-1826 (IL-4 + CpG group) that was supplemented with irradiated syngeneic naive splenocytes (30 Gy, $1x10^6$ cells/ml) as well as 50 IU/ml recombinant mouse IL-2 (Nippon Becton-Dickinson). Cytolytic assays were performed 6 days after the last stimulation using the responder cells as effector cells. Naïve splenocytes that were stimulated twice *in vitro* with irradiated-IL4 tumor cells and CpG-ODN as described above were used as control effector cells.

Cytolytic assays. Cytolytic assays were performed as previously described (22). Tumor-stimulated effector cells were assessed for cytolytic activity against MC38-WT and YAC-1 cells, which are sensitive to non-specific killing, in triplicate in 4-h ^{51}Cr-release assays. The percentage of lysis was determined using the following formula: (release in assay - spontaneous release) x 100/(maximum release - spontaneous release). Maximum release was determined by the lysis of labeled target cells with 1% Triton X-100. Spontaneous release, which was measured by incubating target cells in the absence of effector cells, was <10% of maximum release.

Statistical analyses. Significance was assessed by Student's t-tests. Differences between groups were considered significant when the P-value was <0.05.

Results

Maturation of DCs was induced by coincubation with IL-4-overexpressing tumor cells and CpG-ODN. We investigated the effects of IL-4 and CpG-ODN on DC maturation by flow cytometry. While the coincubation of DCs with MC38-IL4

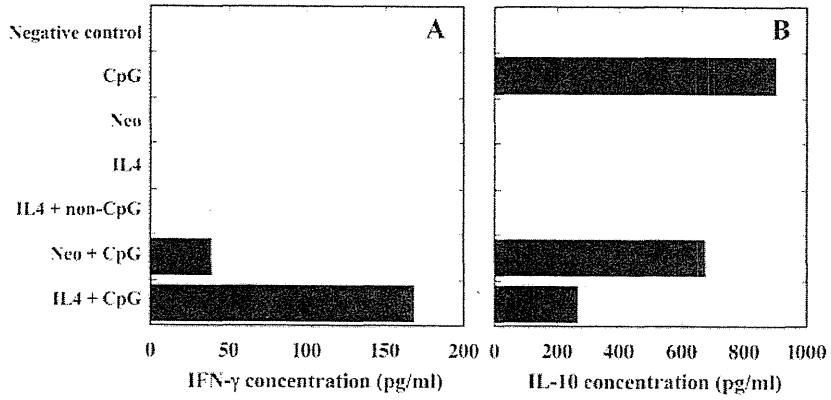

Figure 2. Type-1 T-helper (Th1) cytokine production by naïve splenocytes is enhanced by coincubation with IL-4 and CpG-ODN. Splenocytes from naive mice were stimulated with IL-4-overexpressing or control gene-transduced MC38 cells either alone or in combination with CpG-ODN-1826 or ODN-1911 *in vitro*. After a 24-h incubation, we measured interferon (IFN)-γ and IL-10 concentrations in the culture supernatant by enzyme-linked immunosorbent assay (ELISA).

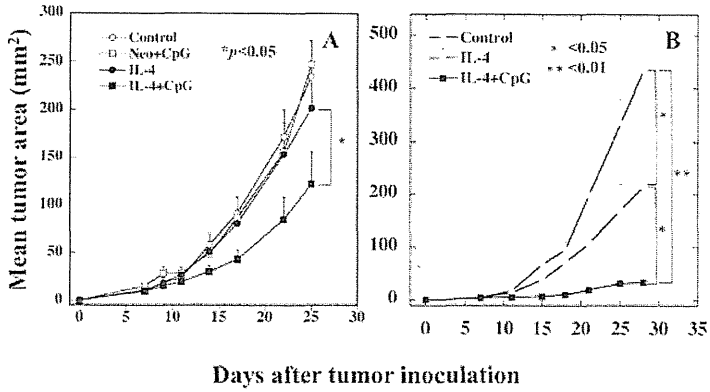

Figure 3. The therapeutic inoculation of IL-4 and CpG-ODN suppresses the growth of parental tumors *in vivo*. B6 mice were injected with MC38-WT cells in the right flank. (A) Seven, 9 and 11 days after the WT inoculation, $3x10^5$ cells/mouse MC38-Neo (Control; open circles), MC38-IL4 cells with 30 μg/mouse CpG-ODN-1826 (Neo + CpG; open squares), MC38-IL4 cells with ODN-1911 (IL-4; closed circle), or MC38-IL-4 cells with CpG-ODN-1826 (IL-4 + CpG; closed squares) were inoculated around the established parental tumors, which had reached 4-20 mm^2 in size. (B) Otherwise, tumor-bearing B6 mice were inoculated $5x10^5$ cells/mouse MC38-Neo (Control; open circles) or MC38-IL4 cells with either ODN-1911 (IL-4; open squares) or CpG-ODN-1826 (IL-4 + CpG; closed squares) were inoculated in the same manner. Tumor size was measured twice a week. Results are reported as mean tumor area (mm^2) ± SE. Significance at 95% confidence limits is indicated.

enhanced the expression of MHC class I, class II, and costimulatory molecules, only minimal phenotypic changes in DCs were detected after coincubation with CpG-ODN. When we compared DCs that were incubated with IL-4-overexpressing MC38 cells and CpG-ODN-1826 (DC + CpG + IL-4) with the other groups, the expression of H-$2K^b$, I-A^b, CD80, and CD86 molecules on the DCs was clearly upregulated (Fig. 1). These results suggest that IL-4 and CpG-ODN have synergistic effects on DC maturation.

The combination of IL-4-overexpressing MC38 cells and CpG-ODN promotes the production of Th1-type cytokines by naïve splenocytes in vitro. Since the combination of IL-4 and CpG-ODN enhanced DC maturation, we observed their effects on naïve splenocytes. ELISAs confirmed that naïve splenocytes produced high amounts of IFN-γ after a 24-h coincubation with MC38-IL4 and CpG-ODN-1826 (Fig. 2A), whereas IFN-γ production could not be detected after coincubation with either IL-4 or CpG-ODN alone. While IL-10 production was clearly detected when naïve splenocytes were incubated with CpG-ODN (Fig. 2B), coincubation with MC38-IL4 suppressed the production of IL-10. These results suggest that the combination of IL-4 and CpG-ODN promoted Th1-type immune responses.

Therapeutic inoculation of IL-4-overexpressing MC38 cells and CpG-ODN reduces the outgrowth of established tumors in vivo. Next, we observed whether CpG-ODN had additive antitumor effects on the effects of IL-4 on established tumors *in vivo*. We treated tumor-bearing mice with MC38-IL4 and CpG-ODN-1826 and compared the parental tumor size. As shown in Fig. 3A, the combination therapy of MC38-IL4 ($3x10^5$ cells/mouse) and CpG-ODN (30 μg/mouse) significantly reduced the outgrowth of the parental tumors (IL-4 vs. IL-4 + CpG, P=0.048) whereas treatment with MC38-Neo + CpG and MC38-IL4 + non-CpG did not show any antitumor effects. Furthermore, the combination of increased cell number of MC38-IL4 ($5x10^5$ cells/mouse)

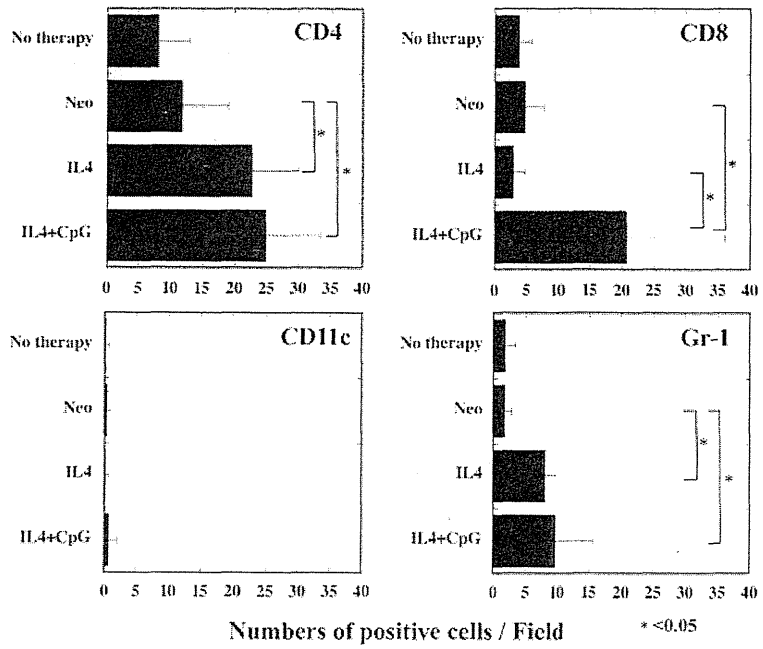

Figure 4. CD8⁺ cells significantly infiltrate the established wild-type (WT) tumors of mice treated with MC38-IL4 and CpG-ODN. B6 mice were injected with either MC38-Neo or MC38-IL4 cells with or without CpG-ODN-1826 in the area surrounding the established WT tumor 7 days after inoculation of MC38-WT cells. Tumor tissues were harvested 3 days after inoculation of the genetically modified tumor and immediately embedded in optimal cutting temperature compound and frozen for sectioning. Serial 5-μm sections were exposed to anti-Gr-1, anti-CD11c, anti-CD4, or anti-CD8a antibodies. Rat IgG2a was used as a control antibody. Immunostaining was completed with a Vectastain ABC kit. Immunoreactive cells were counted in 6 fields in a light microscope (magnification, x400) in a blinded fashion. Results are shown as mean numbers of positive cells/field ± SD.

and CpG-ODN (30 μg/mouse) was more effective against the established tumors (Fig. 3B; IL-4 vs. IL-4 + CpG, P=0.015) while treatment with MC38-IL4 ($5x10^5$ cells/mouse) only also revealed antitumor activity. Therefore, the combination therapy of IL-4 and CpG-ODN has an additive antitumor effect *in vivo*.

Treatment of IL-4-overexpressing MC38 cells with the combination of CpG-ODN induces the infiltration of CD8-positive cells in established wild-type tumors. We analyzed the mechanisms of the antitumor effects that were induced by the inoculation of MC38-IL4 cells with CpG-ODN-1826. As shown in Fig. 4, WT tumors of mice treated with MC38-IL4 showed significant infiltration with Gr-1⁺ cells, as previously reported (4). More CD4⁺ cells infiltrated tumors in mice treated with MC38-IL4 alone, as well as with MC38-IL4 and CpG-ODN, compared with those in mice treated with MC38-Neo (P=0.039 and P=0.026, respectively). While only a few CD8⁺ cells could be detected in the tumors of mice treated with MC38-IL4 alone, a marked infiltration of CD8⁺ cells was observed in the tumors of mice treated with MC38-IL4 and CpG-ODN (Fig. 4; MC38-IL4 alone: 2.8±1.9 cells/field vs. MC38-IL4 + CpG-ODN, 20.7±15.3 cells/field, P=0.027). CD11c⁺ cells were rarely seen in any of the groups. These results suggest that the initial antitumor effects induced by MC38-IL4 and CpG-ODN may be dependent on CD8⁺ and CD4⁺ cells.

Potent tumor-specific cytolysis is detected when splenocytes of MC38-immune mice are stimulated by the combination of IL-4-overexpressing tumor cells and CpG-ODN. Because the combination of IL-4 and CpG-ODN seemed to induce potent Th1-type immune responses, we tried to detect the generation of tumor-specific CTL in mice immunized with IL-4 and CpG-ODN. As shown in Fig. 5, effector cells that were stimu-

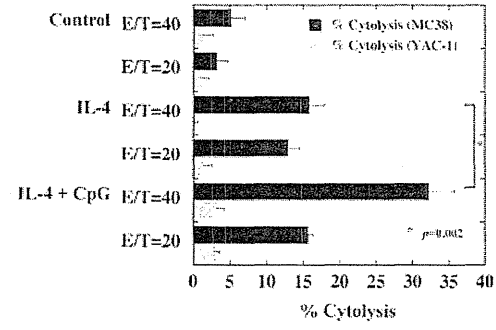

Figure 5. Stimulation with MC38-IL4 and CpG-ODN induces potent tumor-specific cytolysis. Immune mice received injections of both MC38-IL4 cells and control-ODN-1911 (IL-4) or MC38-IL4 cells in combination with CpG-ODN-1826 (IL4 + CpG) on Day 0 and MC38-WT cells on Days 7 and 28. Splenocytes from immunized mice were harvested on Day 42 and stimulated *in vitro* with irradiated MC38-IL4 tumor cells either alone (IL-4) or in combination with CpG-ODN-1826 (IL4 + CpG). Seven days later, responder cells were restimulated with irradiated-IL4 tumor cells either alone (IL-4) or in combination with CpG-ODN-1826 (IL4 + CpG) and supplemented with irradiated syngeneic naive splenocytes as well as recombinant mouse IL-2. Naïve splenocytes that were stimulated with irradiated-IL4 tumor cells and CpG-ODN as described above were also used as control effector cells (Control). A cytolytic assay (4h-^{51}Cr-release assay) against MC38 or YAC-1 cells was performed 6 days after the second stimulation. Results are reported as mean % cytotoxicity ± SD. E:T, effector to target.

lated with IL-4 and CpG-ODN revealed marked cytolysis that was specific for MC38-WT cells (32.2±3.5% for MC38 vs. 3.2±1.1% for YAC-1; at effector to target ratio, E:T=40). Although tumor-specific cytolysis was also detected when the splenocytes of immunized mice that had been inoculated with MC38-IL4 cells and non-CpG-ODN-1911 *in vivo* were stimulated with MC38-IL4 cells *in vitro*, the specific lysis was lower compared to that of the splenocytes of mice treated with IL-4 and CpG-ODN (15.8±2.1% for MC38 vs. 0.3±0.3% for YAC-1; E:T=40, P=0.002 when compared with IL4 + CpG for lysis of MC38). Naïve splenocytes stimulated with IL-4 + CpG-ODN did not show any MC38-specific killing (Fig. 5). The results suggested that immunization with IL-4 and CpG-ODN effectively induce tumor-specific immune response *in vivo*.

Discussion

In this study, we observed that the combination of IL-4 and CpG-ODN enhanced the expression of MHC and costimulatory molecules on the surface of DCs. In addition, the combination promoted IFN-γ production and suppressed IL-10 production in naïve splenocytes *in vitro*, which strongly suggested that the combination of IL-4 and CpG-ODN contributed to T-cell differentiation towards a Th1-type immune response. The combined therapy of IL-4 and CpG effectively suppressed the outgrowth of parental tumors *in vivo* compared to IL-4 monotherapy. The results of both the immunohistochemical and the tumor-specific cytolysis analyses suggested that Th1-type immune responses were strongly induced in mice treated with IL-4 and CpG-ODN.

IL-4, which is a representative Th2-type cytokine, is produced by Th2-type cells. The Th2-type response is thought to suppress the generation of Th1 cells (23), which are usually involved in antitumor immunity. However, it has been reported that IL-4 shows multiple suppressive effects on tumors, and our previous investigation showed that IL-4 gene transduction in MC38 cells did not affect *in vitro* tumor growth, while tumors were not seen in most mice injected with IL-4-overexpressing MC38 cells. This observation implies that IL-4 does not injure MC38 cells directly but reduces their tumorigenicity by inducing host immune responses. Our previous study and other investigations have suggested that IL-4 recruits and activates granulocytes in the microenvironment of parental tumors in order to attack and kill the tumor cells during the primary response. However, how IL-4 recruits or stimulates granulocytes in the tumor microenvironment remains unclear (4,24). Thus, IL-4 induces tumor-specific cellular immune responses, which contribute to long-lasting immunity against the parental tumors.

For further improvement of the antitumor effects of IL-4-based immune therapy, we performed combination therapy, which consisted of IL-4 with CpG-ODN, and this combination has been reported as a potent inducer of immune responses. As previously reported, treatment with CpG-ODN alone did not reduce tumor outgrowth (3). Although CpG-ODN is thought to promote the induction of Th1-type cytokines, CpG-ODN promoted IL-10 production by naïve splenocytes in our system. Reports show that CpG induces Th2-type cytokines in certain conditions support our observation (25,26). MC38-IL4 did not promote IL-10 production, whereas exogenous IL-4 might. We speculate that irradiated tumor cells modified the immune circumstances in the culture. In any case, we suggest that the balance of Th1/Th2 cytokine production is critical to the induction of potent immune responses in the early stages of tumor development and that the great suppression of outgrowth of the parental tumors that was seen in this study occurred because the combination of IL-4 and CpG enhanced IFN-γ production and suppressed IL-10 production. Further investigation is required in order to clarify the mechanisms by which IL-4 reduces the IL-10 production that is induced by CpG.

However, opposite effects of IL-4 on tumors have also been reported. IL-4 itself may affect tumor growth, especially on those that have abundant IL-4 receptors. The levels of expression of the IL-4 receptor correlated with the tumorigenic potential in a murine model (27). Several tumors appeared to be resistant to apoptosis, which is induced by chemotherapeutic agents or CD95 ligation, in an IL-4-dependent manner. IL-4 seemed to modify the immunological functions of effector cells. The cultivation of naïve $CD8^+$ T cells in the presence of IL-4 resulted in poor cytolytic function in the cells by reducing the levels of perforin and granzymes (27,28). Whether an immune response is predominantly Th1 or Th2 may depend on a number of other factors, such as mouse strain, kind of tumor, amount of tumor antigen, and the amount of cytokine (29,30).

It has been reported that the combination of CpG, IL-4, and CD40 ligand effectively induce CTLs by enhancing the expression of immunogenic molecules on B-cell precursor acute lymphoblastic leukemia cells (31). Although MHC class I molecules were slightly upregulated by IL-4 transduction in MC38 cells, changes in other molecules, such as costimulatory and MHC class II molecules, could not be detected in our system (unpublished data). It was thought that IL-4 and CpG-ODN resulted in antitumor effects by inducing Th1-type immune responses, especially that of tumor-specific CTLs, rather than by modulating the immunogenic molecules in the tumor cells. The mechanism by which cytokines and immunomodulators exhibit antitumor effects may also depend on the models used in the experiments.

In order to perform tumor-based gene therapy, there are a number of issues, such as dose determination, site of therapeutic injection, and therapeutic interval, that need to be determined, but the most critical issue is the establishment of the patient's cytokine gene-transduced tumor cells. The development of a new technique that transduces a targeted gene to a patient's cells may be required.

Finally, we found in this study that combination therapy with IL-4 and CpG-ODN had potent antitumor effects on established tumors through the induction of potent Th1-type immune responses in the hosts. Thus, this combination therapy may be a candidate for clinical cancer therapy, but further investigation is needed before clinical trials.

Acknowledgements

This study was supported in part by a grant from the Ministry of Health, Labor, and Welfare of Japan (K. Hiroishi); a Grant-in-Aid for Scientific Research (C) from the Ministry of Education, Culture, Sports, Science and Technology of

Japan (K. Hiroishi); a grant for the High-Technology Research Center Project from the Ministry of Education, Culture, Sports, Science, and Technology of Japan (M. Imawari); and the Research Program of Intractable Disease provided by the Ministry of Health, Labor and Welfare of Japan (K. Hiroishi).

References

1. Eguchi J, Hiroishi K, Ishii S and Mitamura K: Interferon-alpha and interleukin-12 gene therapy of cancer: interferon-alpha induces tumor-specific immune responses while interleukin-12 stimulates non-specific killing. Cancer Immunol Immunother 52: 378-386, 2003.
2. Ishii S, Hiroishi K, Eguchi J, Hiraide A and Imawari M: Dendritic cell therapy with interferon-alpha synergistically suppresses outgrowth of established tumors in a murine colorectal cancer model. Gene Ther 13: 78-87, 2006.
3. Hiraide A, Hiroishi K, Eguchi J, Ishii S, Doi H and Imawari M: Dendritic cells stimulated with cytidine-phosphate-guanosine oligodeoxynucleotides and interferon-alpha-expressing tumor cells effectively reduce outgrowth of established tumors in vivo. Cancer Sci 99: 1663-1669, 2008.
4. Eguchi J, Hiroishi K, Ishii S, *et al*: Interleukin-4 gene transduced tumor cells promote a potent tumor-specific Th1-type response in cooperation with interferon-alpha transduction. Gene Ther 12: 733-741, 2005.
5. Seder RA, Paul WE, Davis MM and Fazekas de St Groth B: The presence of interleukin 4 during in vitro priming determines the lymphokine-producing potential of CD4+ T cells from T cell receptor transgenic mice. J Exp Med 176: 1091-1098, 1992.
6. Hsieh CS, Heimberger AB, Gold JS, O'Garra A and Murphy KM: Differential regulation of T helper phenotype development by interleukins 4 and 10 in an alpha beta T-cell-receptor transgenic system. Proc Natl Acad Sci USA 89: 6065-6069, 1992.
7. Paul WE: Interleukin 4/B cell stimulatory factor 1: one lymphokine, many functions. FASEB J 1: 456-461, 1987.
8. Li Z, Chen L and Qin Z: Paradoxical roles of IL-4 in tumor immunity. Cell Mol Immunol 6: 415-422, 2009.
9. Toi M, Bicknell R and Harris AL: Inhibition of colon and breast carcinoma cell growth by interleukin-4. Cancer Res 52: 275-279, 1992.
10. Obiri NI, Hillman GG, Haas GP, Sud S and Puri RK: Expression of high affinity interleukin-4 receptors on human renal cell carcinoma cells and inhibition of tumor cell growth in vitro by interleukin-4. J Clin Invest 91: 88-93, 1993.
11. Volpert OV, Fong T, Koch AE, *et al*: Inhibition of angiogenesis by interleukin 4. J Exp Med 188: 1039-1046, 1998.
12. Rosenman SJ, Shrikant P, Dubb L, Benveniste EN and Ransohoff RM: Cytokine-induced expression of vascular cell adhesion molecule-1 (VCAM-1) by astrocytes and astrocytoma cell lines. J Immunol 154: 1888-1899, 1995.
13. Yu JS, Wei MX, Chiocca EA, Martuza RL and Tepper RI: Treatment of glioma by engineered interleukin 4-secreting cells. Cancer Res 53: 3125-3128, 1993.
14. Benedetti S, Dimeco F, Pollo B, *et al*: Limited efficacy of the HSV-TK/GCV system for gene therapy of malignant gliomas and perspectives for the combined transduction of the interleukin-4 gene. Hum Gene Ther 8: 1345-1353, 1997.
15. Saleh M, Wiegmans A, Malone Q, Stylli SS and Kaye AH: Effect of in situ retroviral interleukin-4 transfer on established intracranial tumors. J Natl Cancer Inst 91: 438-445, 1999.
16. Eguchi J, Kuwashima N, Hatano M, *et al*: IL-4-transfected tumor cell vaccines activate tumor-infiltrating dendritic cells and promote type-1 immunity. J Immunol 174: 7194-7201, 2005.
17. Okada H, Lieberman FS, Walter KA, *et al*: Autologous glioma cell vaccine admixed with interleukin-4 gene transfected fibroblasts in the treatment of patients with malignant gliomas. J Transl Med 5: 67, 2007.
18. Kurtz DM, Tschetter LK, Allred JB, *et al*: Subcutaneous interleukin-4 (IL-4) for relapsed and resistant non-Hodgkin lymphoma: a phase II trial in the North Central Cancer Treatment Group, NCCTG 91-78-51. Leuk Lymphoma 48: 1290-1298, 2007.
19. Hiraide A, Hiroishi K, Ishii S, Eguchi J and Imawari M: Cytidine-phosphate-guanosine oligodeoxynucleotides and interferon-alpha-expressing tumor cells effectively induce dendritic cell maturation in vitro. Anticancer Res 26: 211-218, 2006.
20. Pear WS, Nolan GP, Scott ML and Baltimore D: Production of high-titer helper-free retroviruses by transient transfection. Proc Natl Acad Sci USA 90: 8392-8396, 1993.
21. Hiroishi K, Tuting T, Tahara H and Lotze MT: Interferon-alpha gene therapy in combination with CD80 transduction reduces tumorigenicity and growth of established tumor in poorly immunogenic tumor models. Gene Ther 6: 1988-1994, 1999.
22. Hiroishi K, Tuting T and Lotze MT: IFN-alpha-expressing tumor cells enhance generation and promote survival of tumor-specific CTLs. J Immunol 164: 567-572, 2000.
23. Sher A and Coffman RL: Regulation of immunity to parasites by T cells and T cell-derived cytokines. Annu Rev Immunol 10: 385-409, 1992.
24. Noffz G, Qin Z, Kopf M and Blankenstein T: Neutrophils but not eosinophils are involved in growth suppression of IL-4-secreting tumors. J Immunol 160: 345-350, 1998.
25. Triozzi PL, Aldrich W and Ponnazhagan S: Regulation of the activity of an adeno-associated virus vector cancer vaccine administered with synthetic Toll-like receptor agonists. Vaccine 28: 7837-7843, 2010.
26. Fitzner N, Zahner L, Habich C and Kolb-Bachofen V: Stimulatory type A CpG-DNA induces a Th2-like response in human endothelial cells. Int Immunopharmacol 11: 1789-1795, 2011.
27. Li Z, Jiang J, Wang Z, *et al*: Endogenous interleukin-4 promotes tumor development by increasing tumor cell resistance to apoptosis. Cancer Res 68: 8687-8694, 2008.
28. Kienzle N, Olver S, Buttigieg K, *et al*: Progressive differentiation and commitment of CD8+ T cells to a poorly cytolytic CD8low phenotype in the presence of IL-4. J Immunol 174: 2021-2029, 2005.
29. Allen JE and Maizels RM: Th1-Th2: reliable paradigm or dangerous dogma? Immunol Today 18: 387-392, 1997.
30. Schuler T, Qin Z, Ibe S, Noben-Trauth N and Blankenstein T: T helper cell type 1-associated and cytotoxic T lymphocyte-mediated tumor immunity is impaired in interleukin 4-deficient mice. J Exp Med 189: 803-810, 1999.
31. Fabricius D, Breckerbohm L, Vollmer A, *et al*: Acute lymphoblastic leukemia cells treated with CpG oligodeoxynucleotides, IL-4 and CD40 ligand facilitate enhanced anti-leukemic CTL responses. Leukemia 25: 1111-1121, 2011.

HEPATOLOGY
Official Journal of the American Association for the Study of Liver Diseases

Discrete Nature of EpCAM$^+$ and CD90$^+$ Cancer Stem Cells in Human Hepatocellular Carcinoma

Taro Yamashita,[1] Masao Honda,[1] Yasunari Nakamoto,[1] Masayo Baba,[1] Kouki Nio,[1] Yasumasa Hara,[1] Sha Sha Zeng,[1] Takehiro Hayashi,[1] Mitsumasa Kondo,[1] Hajime Takatori,[1] Tatsuya Yamashita,[1] Eishiro Mizukoshi,[1] Hiroko Ikeda,[1] Yoh Zen,[1] Hiroyuki Takamura,[1] Xin Wei Wang,[2] and Shuichi Kaneko[1]

Recent evidence suggests that hepatocellular carcinoma (HCC) is organized by a subset of cells with stem cell features (cancer stem cells; CSCs). CSCs are considered a pivotal target for the eradication of cancer, and liver CSCs have been identified by the use of various stem cell markers. However, little information is known about the expression patterns and characteristics of marker-positive CSCs, hampering the development of personalized CSC-targeted therapy. Here, we show that CSC markers EpCAM and CD90 are independently expressed in liver cancer. In primary HCC, EpCAM$^+$ and CD90$^+$ cells resided distinctively, and gene-expression analysis of sorted cells suggested that EpCAM$^+$ cells had features of epithelial cells, whereas CD90$^+$ cells had those of vascular endothelial cells. Clinicopathological analysis indicated that the presence of EpCAM$^+$ cells was associated with poorly differentiated morphology and high serum alpha-fetoprotein (AFP), whereas the presence of CD90$^+$ cells was associated with a high incidence of distant organ metastasis. Serial xenotransplantation of EpCAM$^+$/CD90$^+$ cells from primary HCCs in immunedeficient mice revealed rapid growth of EpCAM$^+$ cells in the subcutaneous lesion and a highly metastatic capacity of CD90$^+$ cells in the lung. In cell lines, CD90$^+$ cells showed abundant expression of c-Kit and *in vitro* chemosensitivity to imatinib mesylate. Furthermore, CD90$^+$ cells enhanced the motility of EpCAM$^+$ cells when cocultured *in vitro* through the activation of transforming growth factor beta (TGF-β) signaling, whereas imatinib mesylate suppressed *TGFB1* expression in CD90$^+$ cells as well as CD90$^+$ cell-induced motility of EpCAM$^+$ cells. *Conclusion*: Our data suggest the discrete nature and potential interaction of EpCAM$^+$ and CD90$^+$ CSCs with specific gene-expression patterns and chemosensitivity to molecular targeted therapy. The presence of distinct CSCs may determine the clinical outcome of HCC. (HEPATOLOGY 2012;00:000–000)

The cancer stem cell (CSC) hypothesis, which suggests that a subset of cells bearing stem-cell–like features is indispensable for tumor development, has recently been put forward subsequent to advances in molecular and stem cell biology. Liver cancer, including hepatocellular carcinoma (HCC), is a leading cause of cancer death worldwide.[1] Recent studies have shown the existence of CSCs in liver cancer cell lines and primary HCC specimens using various stem cell markers.[2-7] Independently, we have identified novel HCC subtypes defined by the hepatic stem/progenitor cell markers,

Abbreviations: 5-FU, fluorouracil; Abs, antibodies; AFP, alpha-fetoprotein; CK-19, cytokeratin-19; CSC, cancer stem cell; DNs, dysplastic nodules; EMT, epithelial mesenchymal transition; EpCAM; epithelial cell adhesion molecule; FACS, fluorescent-activated cell sorting; HBV, hepatitis B virus; HCC, hepatocellular carcinoma; HCV, hepatitis C virus; HSCs, hepatic stem cells; IF, immunofluorescence; IHC, immunohistochemistry; IR, immunoreactivity; MDS, multidimensional scaling; NBNC, non-B, non-C hepatitis; NOD/SCID, nonobese diabetic, severe combined immunodeficient; NT, nontumor; OV-1, ovalbumin 1; qPCR, quantitative real-time polymerase chain reaction; SC, subcutaneous; Smad3, Mothers against decapentaplegic homolog 3; TECs, tumor epithelial cells; TGF-β, transforming growth factor beta; T/N, tumor/nontumor; VECs, vascular endothelial cells; VM, vasculogenic mimicry; VEGFR, vascular endothelial growth factor receptor.

From the [1]Liver Center, Kanazawa University Hospital, Kanazawa, Ishikawa, Japan; and [2]Laboratory of Human Carcinogenesis, Center for Cancer Research, National Cancer Institute, Bethesda, MD.

Received July 9, 2012; revised October 22, 2012; accepted November 6, 2012.

This study was supported by a Grant-in-Aid from the Ministry of Education, Culture, Sports, Science, and Technology of Japan (23590967), a grant from the Japanese Society of Gastroenterology, a grant from the Ministry of Health, Labor, and Welfare, and a grant from the National Cancer Center Research and Development Fund (23-B-5) of Japan. X.W.W. is supported by the Intramural Research Program of the Center for Cancer Research, U.S. National Cancer Institute.

epithelial cell adhesion molecule (EpCAM) and alpha-fetoprotein (AFP), which correlate with distinct gene-expression signatures and prognosis.[8,9] $EpCAM^+$ HCC cells isolated from primary HCC and cell lines show CSC features, including tumorigenicity, invasiveness, and resistance to fluorouracil (5-FU).[10] Similarly, other groups have shown that $CD133^+$, $CD90^+$, and $CD13^+$ HCC cells are also CSCs, and that EpCAM, CD90, and CD133 are the only markers confirmed to enrich CSCs from primary HCCs thus far.[3-5,10]

Although $EpCAM^+$, $CD90^+$, and $CD133^+$ cells show CSC features, such as high tumorigenicity, an invasive nature, and resistance to chemo- and radiation therapy, it remains unclear whether these cells represent an identical HCC population and whether they share similar or distinct characteristics. In this study, we used fluorescent-activated cell sorting (FACS), microarray, and immunohistochemistry (IHC) techniques to investigate the expression patterns of the representative liver CSC markers CD133, CD90, and EpCAM in a total of 340 HCC cases and 7 cases of mesenchymal liver tumors. We further explored gene- and protein-expression patterns as well as tumorigenic capacity of sorted cells isolated from 15 primary HCCs and 7 liver cancer cell lines in an attempt to identify the molecular portraits of each cell type.

Materials and Methods

Clinical Specimens. HCC samples were obtained with informed consent from patients who had undergone radical resection at the Liver Center in Kanazawa University Hospital (Kanazawa, Japan), and tissue acquisition procedures were approved by the ethics committee of Kanazawa University. A total of 102 formalin-fixed and paraffin-embedded HCC samples, obtained from 2001 to 2007, were used for IHC analyses. Fifteen fresh HCC samples were obtained between 2008 and 2012 from surgically resected specimens and an autopsy specimen and were used immediately to prepare single-cell suspensions and xenotransplantation (Table 1). Seven hepatic stromal tumors (three cavernous hemangioma, two hemangioendothelioma, and two angiomyolipoma) were formalin fixed and paraffin embedded and used for IHC analyses.

Table 1. Clinicopathological Characteristics of HCC Cases Used for Xenotransplantation

ID	Age/ Sex	Etiology	Tumor Size (cm)	Histological Grade	AFP (ng/mL)	DCP (IU/mL)
P1	77/M	Alcohol	12.0	Moderate	198	322
P2	61/F	NBNC	11.0	Moderate	12	3,291
P3	66/M	NBNC	2.2	Moderate	13	45
P4	65/M	HCV	4.2	Poor	13,700	25,977
P5	52/M	HBV	6.0	Moderate	29,830	1,177
P6	60/M	HCV	2.7	Poor	249	185
P7	79/F	HBV	4.0	Poor	46,410	384
P8	77/F	NBNC	5.5	Moderate	17,590	562
P9	71/M	Alcohol	7.0	Poor	3,814	607
P10	51/M	HBV	2.2	Well	<10	21
P11	71/M	Alcohol	2.1	Well	<10	11
P12	60/M	HBV	10.8	Poor	323	2,359
P13	66/M	HCV	2.8	Moderate	11	29
P14	71/M	HCV	7.2	Moderate	235,700	375,080
P15	75/M	HBV	5.5	Poor	<10	97

Abbreviation: DCP, des-gamma-carboxy prothrombin.

Additional details of experimental procedures are available in the Supporting Information.

Results

EpCAM, CD133, and CD90 Expression in HCC. We first evaluated the frequencies of three representative CSC markers ($EpCAM^+$, $CD90^+$, and $CD133^+$ cells) in 12 fresh primary HCC cases surgically resected by FACS (representative data shown in Fig. 1A). Clinicopathological characteristics of primary HCC cases are shown in Table 1. We noted that frequency of $EpCAM^+$, $CD90^+$, and $CD133^+$ cells varied between individuals. Abundant $CD90^+$ (7.0%), but almost no $EpCAM^+$, cells (0.06%, comparable to the isotype control) were detected in P2, whereas few $CD90^+$ (0.6%), but abundant $EpCAM^+$, cells (17.5%) were detected in P4. Very small populations of $EpCAM^+$ (0.09%), $CD90^+$ (0.04%), and $CD133^+$ cells (0.05%) were found in P12, but they were almost nonexistent in P8, except for $CD90^+$ cells (0.08%) (Fig. 1A). We further evaluated the expression of EpCAM, CD90, and CD133 in xenografts obtained from surgically resected samples (P13 and P15) and an autopsy sample (P14). As a whole, compared to the isotype control, 7 of 15 HCCs contained definite $EpCAM^+$ cells (46.7%), whereas only 3 HCCs

Address reprint requests to: Taro Yamashita, M.D., Ph.D., Department of General Medicine, Kanazawa University Hospital, 13-1 Takara-Machi, Kanazawa, Ishikawa 920-8641, Japan. E-mail: taroy@m-kanazawa.jp; fax: +81-76-234-4250.

View this article online at wileyonlinelibrary.com.
DOI 10.1002/hep.26168
Potential conflict of interest: Nothing to report.
Additional Supporting Information may be found in the online version of this article.

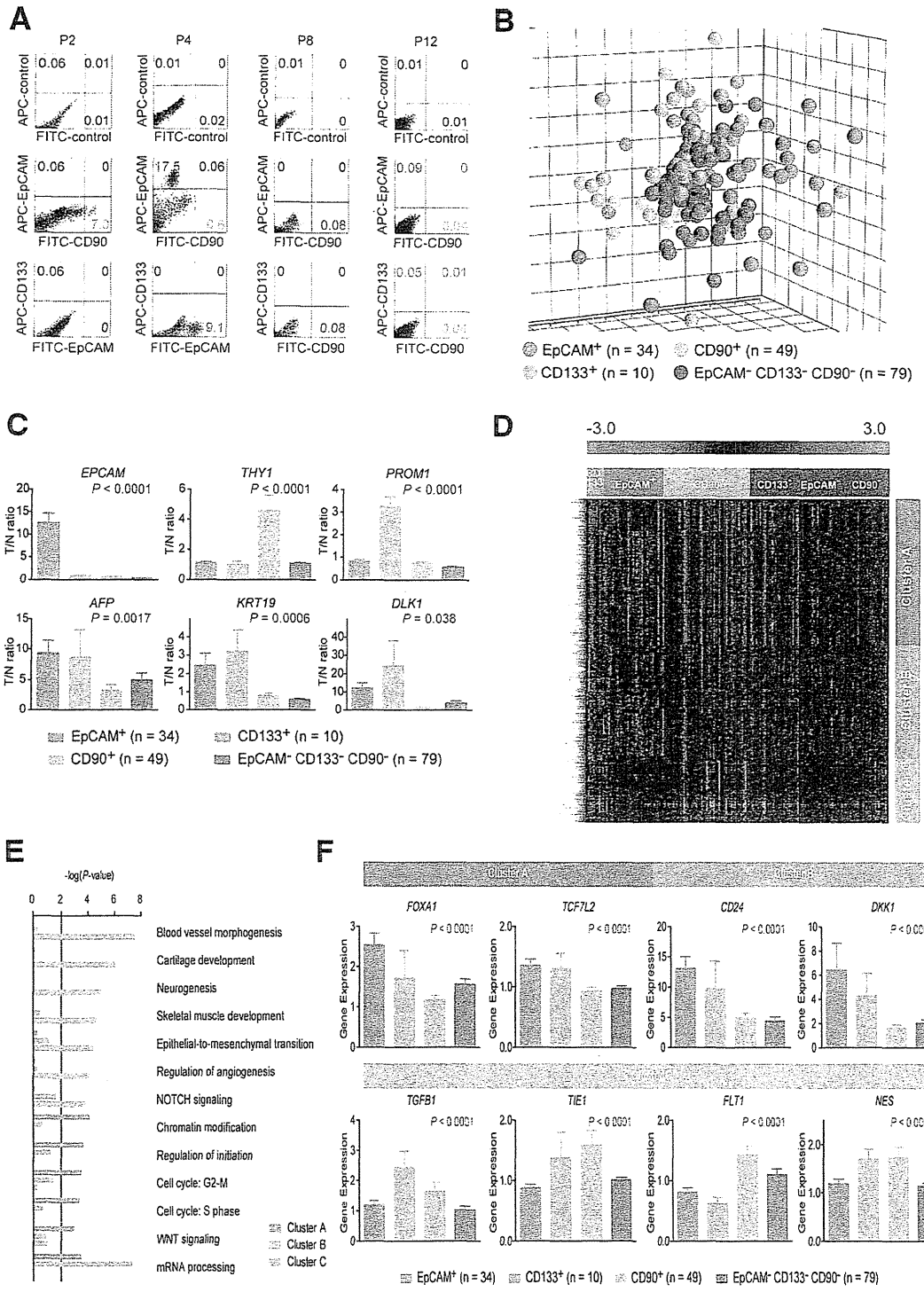

Fig. 1. Gene-expression profiles of CSC marker-positive HCCs. (A) FACS analysis of primary HCCs stained with fluorescent-labeled Abs against EpCAM, CD90, or CD133. (B) Multidimensional scaling analysis of 172 HCC cases characterized by the expression patterns of EpCAM, CD133, and CD90. Red, EpCAM$^+$ CD90$^-$ CD133$^-$ (n = 34); orange, EpCAM$^-$ CD90$^-$ CD133$^+$ (n = 10); light blue, EpCAM$^-$ CD90$^+$ CD133$^-$ (n = 49); blue, EpCAM$^-$ CD90$^-$ CD133$^-$ (n = 79). HCC specimens were clustered in specific groups with statistical significance ($P < 0.001$). (C) Expression patterns of well-known hepatic stem/progenitor markers in each HCC subtype, as analyzed by microarray. Red bar, EpCAM$^+$; orange bar, CD133$^+$; light blue bar, CD90$^+$; blue bar, EpCAM$^-$ CD90$^-$ CD133$^-$. (D) Hierarchical cluster analysis based on 1,561 EpCAM/CD90/CD133-coregulated genes in 172 HCC cases. Each cell in the matrix represents the expression level of a gene in an individual sample. Red and green cells depict high and low expression levels, respectively, as indicated by the scale bar. (E) Pathway analysis of EpCAM/CD90/CD133-coregulated genes. Canonical signaling pathways activated in cluster A (red bar), cluster B (orange bar), or cluster C (light blue bar) with statistical significance ($P < 0.01$) are shown. (F) Expression patterns of representative genes differentially expressed in EpCAM/CD90/CD133 HCC subtypes. Red bar, EpCAM$^+$; orange bar, CD133$^+$; light blue bar, CD90$^+$; blue bar, EpCAM$^-$ CD133$^-$ CD90$^-$.

Table 2. Tumorigenic Capacity of Unsorted, EpCAM$^+$, EpCAM$^-$, CD90$^+$, and CD90$^-$ Cells From Primary HCCs and Xenografts

Sample	CD133 (%)	CD90 (%)	EpCAM (%)	Cell Surface Marker	Number of Cells	Tumor Formation 2M	Tumor Formation 3M
P1	0	3.1	0	Unsorted	1×10^7	0/5	0/5
				CD90$^+$	1×10^5	0/5	0/5
				CD90$^-$	1×10^5	0/5	0/5
P2	0.06	7.0	0.06	Unsorted	1×10^7	0/5	0/5
				CD90$^+$	1×10^5	0/5	0/5
				CD90$^-$	1×10^5	0/5	0/5
P3	0	1.3	0	Unsorted	1×10^6	0/2	0/2
				CD90$^+$	1×10^4	0/4	0/4
				CD90$^-$	1×10^4	0/4	0/4
P4	0	0.6	17.5	Unsorted	1×10^6	3/4	4/4
				EpCAM$^+$	1×10^3	0/3	2/3
					1×10^4	3/4	4/4
					1×10^5	3/3	3/3
				CD90$^+$	1×10^3	0/3	0/3
					1×10^4	0/4	0/4
					1×10^5	0/3	0/3
				EpCAM$^-$ CD90$^-$	1×10^3	0/3	0/3
					1×10^4	0/4	0/4
					1×10^5	0/3	0/3
P5	0	0.8	29.7	Unsorted	1×10^6	0/5	0/5
				EpCAM$^+$	1×10^5	0/5	0/5
				CD90$^+$	1×10^5	0/5	0/5
				EpCAM$^-$ CD90$^-$	1×10^5	0/5	0/5
P6	0	0.7	0	Unsorted	1×10^6	0/2	0/2
				CD90$^+$	1×10^4	0/4	0/4
				CD90$^-$	1×10^4	0/4	0/4
P7	1.38	4.5	4.4	Unsorted	1×10^6	2/2	2/2
				EpCAM$^+$	2×10^2	0/3	0/3
					1×10^3	0/3	1/3
					1×10^4	2/4	4/4
				CD90$^+$	2×10^2	0/3	0/3
					1×10^3	0/3	0/3
					1×10^4	0/4	0/4
				EpCAM$^-$ CD90$^-$	1×10^3	0/3	0/3
					1×10^4	0/3	0/3
					1×10^5	0/4	0/4
P8	0	0.08	0	Unsorted	1×10^5	0/4	0/4
				CD90$^+$	1×10^3	0/3	0/3
				CD90$^-$	1×10^5	0/3	0/3
P9	0	0.26	0	Unsorted	1×10^5	0/4	0/4
				CD90$^+$	1×10^3	0/3	0/3
				CD90$^-$	1×10^5	0/3	0/3
P10	0	0.78	0	Unsorted	1×10^4	0/4	0/4
				CD90$^+$	1×10^3	0/3	0/3
				CD90$^-$	1×10^4	0/3	0/3
P11	0	0.1	1.54	Unsorted	5×10^4	0/2	0/2
				EpCAM$^+$	1×10^3	0/3	0/3
				CD90$^+$	1×10^3	0/3	0/3
				EpCAM$^-$ CD90$^-$	1×10^4	0/3	0/3
P12	0.06	0.05	0.09	Unsorted	1×10^5	0/3	3/3
				CD90$^+$	1×10^3	0/4	1/4
				CD90$^-$	1×10^3	0/4	1/4
					1×10^4	0/3	3/3
P13	0	0.03	67.7	EpCAM$^+$	5×10^5	4/4	NA
					5×10^4	3/3	NA
					5×10^3	3/3	NA
				EpCAM$^-$	5×10^5	0/4	NA
					5×10^4	0/3	NA
					5×10^3	0/3	NA
P14	24.0	0.06	3.1	EpCAM$^+$	5×10^3	4/5	NA
				EpCAM$^-$	5×10^3	2/5	NA
P15	0	2.45	0	CD90$^+$	5×10^4	3/4	NA
					5×10^3	1/3	NA
					5×10^2	1/3	NA
				CD90$^-$	5×10^4	2/4	NA
					5×10^3	1/3	NA
					5×10^2	0/3	NA

NA, not available.

contained definite CD133$^+$ cells (20%) (Table 2). CD90$^+$ cells were detected at variable frequencies in all 15 HCCs analyzed.

To explore the status of these CSC marker-positive cells in HCC in a large cohort, we utilized oligo-DNA microarray data from 238 HCC cases (GEO accession no.: GSE5975) to evaluate the expression of *EPCAM* (encoding EpCAM and CD326), *THY1* (encoding CD90), and *PROM1* (encoding CD133) in whole HCC tissues and nontumor (NT) tissues. Because previous studies demonstrated that CD133$^+$ and CD90$^+$ cells were detected at low frequency (~13.6% by CD133 staining and ~6.2% by CD90 staining) in HCC, but were almost nonexistent in NT liver (4, 5),[4,5] we utilized tumor/nontumor (T/N) gene-expression ratios to detect the existence of marker-positive CSCs in tumor. Accordingly, we showed that a 2-fold cutoff of T/N ratios of *EPCAM* successfully stratifies HCC samples with EpCAM$^+$ liver CSCs.[9,10]

A total of 95 (39.9%), 110 (46.2%), and 31 (13.0%) of the 238 HCC cases were thus regarded as EpCAM$^+$, CD90$^+$, and CD133$^+$ HCCs (T/N ratios: $\geq$2.0), respectively. As observed in the FACS data described above, we detected coexpression of EpCAM and CD90 in 45 HCCs (18.9%), EpCAM and CD133 in five HCCs (2%), CD90 and CD133 in five HCCs (2%), and EpCAM, CD90, and CD133 in 11 HCCs (4.6%). To clarify the characteristics of gene-expression signatures specific to stem cell marker expression status, we selected 172 HCC cases expressing a single CSC marker (34 EpCAM$^+$ CD90$^-$ CD133$^-$, 49 EpCAM$^-$ CD90$^+$ CD133$^-$, and 10 EpCAM$^-$ CD90$^-$ CD133$^+$) or all marker-negative HCCs (79 EpCAM$^-$ CD90$^-$ CD133$^-$). A class-comparison analysis with

univariate F tests and a global permutation test (×10,000) yielded a total of 1,561 differentially expressed genes. Multidimensional scaling (MDS) analysis using this gene set indicated that HCC specimens were clustered in specific groups with statistical significance ($P < 0.001$). Close examination of MDS plots revealed three major HCC subtype clusters: all marker-negative HCCs (blue spheres); EpCAM single-positive HCCs (red spheres); and CD90 single-positive HCCs (light blue spheres). $CD133^+$ HCCs (orange spheres) were rare, relatively scattered, and not clustered (Fig. 1B).

We examined the expression of representative hepatic stem/progenitor cell markers *AFP*, *KRT19*, and *DLK1* in HCCs with regard to the gene-expression status of each CSC marker (Fig. 1C). All three markers were up-regulated in $EpCAM^+$ and $CD133^+$ HCCs, compared with all marker-negative HCCs, consistent with previous findings.[10,11] However, we found no significant overexpression of *AFP*, *KRT19*, and *DLK1* in $CD90^+$ and all marker-negative HCCs.

Hierarchical cluster analyses revealed three main gene clusters that were up-regulated in $EpCAM^+$ HCCs (cluster A, 706 genes), $EpCAM^+$ or $CD133^+$ HCCs (cluster B, 530 genes), and $CD90^+$ or $CD133^+$ HCCs (cluster C, 325 genes) (Fig. 1D). Pathway analysis indicated that the enriched genes in cluster A (red bar) were associated with chromatin modification, cell-cycle regulation, and Wnt/β-catenin signaling (Fig. 1E). Genes associated with messenger RNA processing were enriched in clusters A (red bar) and B (orange bar). Surprisingly, genes in cluster C were significantly associated with pathways involved in blood-vessel morphogenesis, angiogenesis, neurogenesis, and epithelial mesenchymal transition (EMT) (light blue bar). Close examination of genes in each cluster suggested that known hepatic transcription factors (*FOXA1*), Wnt regulators (*TCF7L2* and *DKK1*), and a hepatic stem cell marker (*CD24*) were dominantly up-regulated in $EpCAM^+$ and $CD133^+$ HCCs (Fig. 1F). By contrast, genes associated with blood-vessel morphogenesis (*TIE1* and *FLT1*), EMT (*TGFB1*), and neurogenesis (*NES*) were activated dominantly in $CD90^+$ HCCs and $CD133^+$ HCCs.

$CD90^+$ HCC Cells Share Features With Mesenchymal Vascular Endothelial Cells. Because $CD133^+$ HCCs were relatively rare and constituted only 13% (microarray cohort) to 20% (FACS cohort) of all HCC samples analyzed, we focused on the characterization of EpCAM and CD90. To clarify the cell identity of $EpCAM^+$ or $CD90^+$ cells in primary HCCs, we performed IHC analysis of 18 needle-biopsy specimens of premalignant dysplastic nodules (DNs), 102 surgically resected HCCs, and corresponding NT liver tissues. When examining the expression of EpCAM and CD90 in cirrhotic liver tissue by double-color IHC analysis, we found that $EpCAM^+$ cells and $CD90^+$ cells were distinctively located and not colocalized (Supporting Fig. 1A). Immunoreactivity (IR) to anti-CD90 antibodies (Abs) was detected in vascular endothelial cells (VECs), inflammatory cells, fibroblasts, and neurons, but not in hepatocytes or cholangiocytes, in the cirrhotic liver (Supporting Fig. 1B, panels a,b). IR to anti-EpCAM Abs was detected in hepatic progenitors adjacent to the periportal area and bile duct epithelial cells in liver cirrhosis (Supporting Fig. 1B, panels c,d).

IR to anti-EpCAM Abs was detected in 37 of 102 surgically resected HCCs (Fig. 2A, panel b), but not in 18 DNs (Fig. 2A, panel a). By contrast, no tumor epithelial cells (TECs) showing IR to anti-CD90 Abs were found in any of the 18 DNs or 102 HCCs examined (Fig. 2A, panels c,d). However, we identified $CD90^+$ cells that were morphologically similar to VECs or fibroblasts within the tumor nodule in 37 of the 102 surgically resected HCC tissues (≥5% positive staining in a given area). IR to anti-CD90 Abs was also detected in hepatic mesenchymal tumors (Supporting Fig. 1C, panels a-c), indicating that CD90 is also a marker of liver stromal tumors.

Double-color IHC and immunofluorescence (IF) analysis confirmed the distinct expression of EpCAM and CD90 in HCC (Fig. 2B), consistent with the FACS data (Fig. 1A). Quantitative real-time polymerase chain reaction (qPCR) analysis of sorted $EpCAM^+$, $CD90^+$, and $EpCAM^-$ $CD90^-$ cells after $CD45^+$ cell depletion indicated that the hepatic stem/progenitor markers, *AFP* and *KRT19*, were up-regulated in $EpCAM^+$ cells (red bar), whereas the mesenchymal markers, *KIT* and *FLT1*, were up-regulated in $CD90^+$ cells (orange bar), compared with $EpCAM^-$ $CD90^-$ cells (blue bar) (Fig. 2C). The hepatocyte marker, *CYP3A4*, was down-regulated in $EpCAM^+$ cells and not detected in $CD90^+$ cells, compared with $EpCAM^-$ $CD90^-$ cells. *POU5F1* and *BMI1* were equally up-regulated in both $EpCAM^+$ and $CD90^+$ cells, compared with $EpCAM^-$ $CD90^-$ cells.

EpCAM and CD90 were independently and distinctively expressed in different cellular lineages, so we evaluated the staining of EpCAM and CD90 separately and analyzed the clinicopathological characteristics of surgically resected HCC cases. HCCs were regarded marker positive if ≥5% positive staining was detected in a given area. The existence of $EpCAM^+$

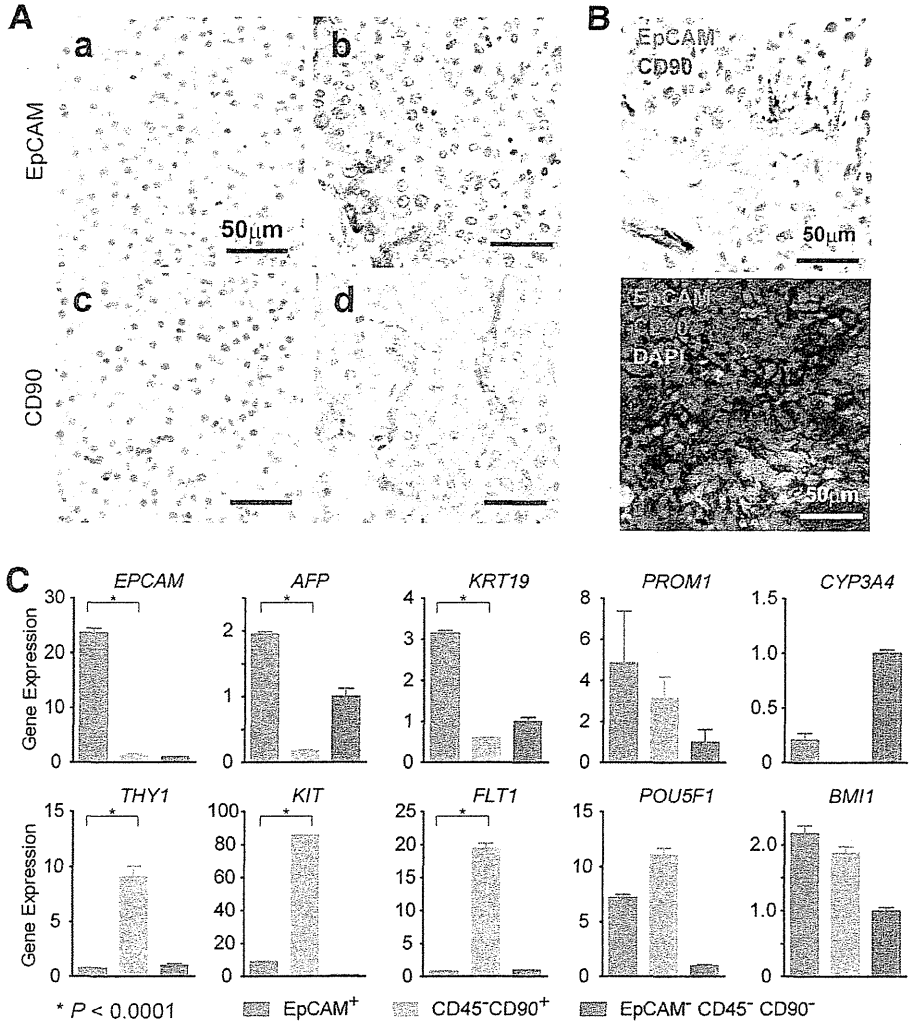

Fig. 2. Distinct EpCAM$^+$ and CD90$^+$ cell populations in HCC. (A) Representative images of EpCAM and CD90 staining in dysplastic nodule (panels a,c) and HCC (panels b,d) by IHC analysis (scale bar, 50 μm). EpCAM (panels a,b) and CD90 (panels c,d) immunostaining is depicted. (B) Upper panel: representative images of EpCAM (red) and CD90 (brown) double staining in HCC by IHC (scale bar, 50 μm). Lower panel: representative images of EpCAM (green) and CD90 (red) staining with 4'6-diamidino-phenylindole (DAPI) (blue) in HCC by IF (scale bar, 50 μm). (C) qPCR analysis of sorted EpCAM$^+$ (red bar), CD90$^+$ (orange bar), or EpCAM$^-$ CD90$^-$ (blue bar) derived from a representative primary HCC. Experiments were performed in triplicate, and data are shown as mean ± standard error of the mean.

cells (≥5%) was characterized by poorly differentiated morphology and high serum AFP values with a tendency for portal vein invasion, whereas the existence of CD90$^+$ cells (≥5%) was associated with poorly differentiated morphology and a tendency for large tumor size (Supporting Tables 2 and 3). Notably, the existence of CD90$^+$ cells was associated with a high incidence of distant organ metastasis, including lung, bone, and adrenal gland, within 2 years after surgery, whereas EpCAM$^+$ cell abundance appeared unrelated to distant organ metastasis.

We evaluated the characteristics of EpCAM$^+$ or CD90$^+$ cells in seven representative HCC cell lines. Morphologically, all EpCAM$^+$ cell lines (HuH1, HuH7, and Hep3B) showed a polygonal, epithelial cell shape, whereas three of four CD90$^+$ cell lines (HLE, HLF, and SK-Hep-1) showed a spindle cell shape (Fig. 3A). EpCAM$^+$ cells were detected in 11.5%, 57.7%, and 99.6% of sorted HuH1, HuH7, and Hep3B cells, respectively. A small CD90$^+$ cell population (0.66%) was observed in PLC/PRL/5, whereas 91.3%, 10.8%, and 59.0% of CD90$^+$ cells were detected in HLE, HLF, and SK-Hep-1, respectively. Compared with primary HCCs, only EpCAM$^+$ or CD90$^+$ cells were detected in liver cancer cell lines under normal culture conditions (Fig. 3B), suggesting that these cell lines contain a relatively pure cell population most likely obtained by clonal selection through the establishment process.

A class-comparison analysis with univariate *t* tests and a global permutation test (×10,000) of microarray data yielded two main gene clusters up-regulated in EpCAM$^+$ cell lines (HuH1, HuH7, and Hep3B) (cluster I, 524 genes) or in CD90$^+$ cell lines (HLE, HLF, and SK-Hep-1) (cluster II, 366 genes) (Fig. 3C). PLC/PRL/5 showed intermediate gene-expression patterns between EpCAM$^+$ and CD90$^+$ cell lines using this gene set. Pathway analysis indicated that the genes

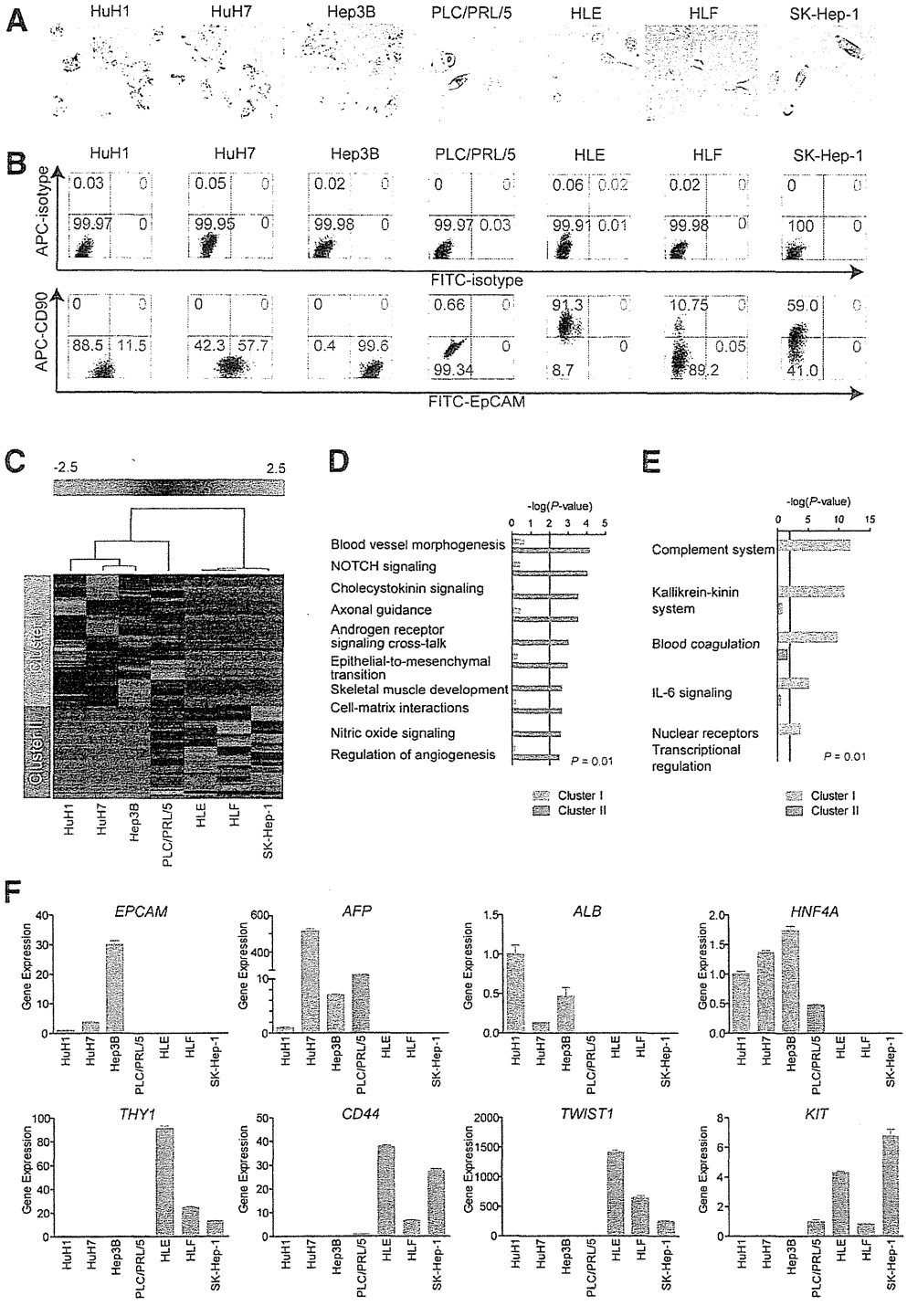

Fig. 3. Characteristics of HCC cell lines defined by EpCAM and CD90. (A) Representative photomicrographs of EpCAM^{+}CD90^{-} and EpCAM^{-} CD90^{+} HCC cell lines. (B) Representative FACS data of EpCAM^{+}CD90^{-} and EpCAM^{-} CD90^{+} HCC cell lines stained with fluorescein isothiocyanate (FITC)-EpCAM and APC-CD90 Abs. (C) Heat-map images of seven HCC cell lines based on 890 EpCAM/CD90-coregulated genes. Each cell in the matrix represents the expression level of a gene in an individual sample. Red and green cells depict high and low expression levels, respectively, as indicated by the scale bar. (D and E) Pathway analysis of EpCAM/CD90-coregulated genes. Canonical signaling pathways activated in cluster I (orange bar) or II (blue bar) with statistical significance ($P < 0.01$) are shown. (F) qPCR of representative differentially expressed genes identified by microarray analysis (C) in seven HCC cell lines.

enriched in cluster II were mainly associated with blood-vessel morpho- and angiogenesis (Fig. 3D). By contrast, the enriched genes in cluster I were significantly associated with known hepatocyte functions ($P < 0.01$) (Fig. 3E). In addition, we identified that the enriched genes in cluster II were significantly associated with neurogenesis, skeletal muscle development, and EMT.

We used qPCR to validate that known hepatic stem cell (HSC) and hepatocyte markers, such as *AFP, EPCAM, ALB*, and *HNF4A* genes, were up-regulated in $EpCAM^+$ cell lines, but not detected in $CD90^+$ cell lines (Fig. 3F). By contrast, genes associated with mesenchymal lineages and EMT, such as *KIT, TWIST1, CD44*, and *THY1*, were strongly up-regulated in $CD90^+$ cell lines.

Unique Tumorigenicity and Metastasis Capacity of Distinct CSCs Defined by EpCAM and CD90. We investigated the tumorigenic capacity of $EpCAM^+$ or $CD90^+$ cells by subcutaneously (SC) injecting 1×10^5 sorted cells of four HCC cell lines (HuH1, HuH7, HLE, and HLF) into nonobese diabetic, severe combined immunodeficient (NOD/SCID) mice. We excluded Hep3B cells for the evaluation of tumorigenicity because almost 100% of cells were EpCAM positive. We further excluded SK-Hep-1 cells from the analysis because they potentially originated from endothelial cells.[12] The highly tumorigenic capacities of $EpCAM^+$ and $CD90^+$ cells were reproduced in HuH1, HuH7, and HLF cell lines, compared with marker-negative cells (Fig. 4A). However, HLE cells did not produce SC tumors, even 12 months after transplantation, in NOD/SCID mice. $EpCAM^+$ cells from HuH1 and HuH7 formed larger tumors more rapidly than $CD90^+$ cells from HLF (Fig. 4B). IHC analyses indicated that $EpCAM^+$ cells did not produce $CD90^+$ cells and *vice versa* in these cell lines *in vivo* (Fig. 4C). $CD90^+$ cells showed a high metastatic capacity, whereas $EpCAM^+$ cells showed no metastasis to the lung when SC tumor volume reached approximately 2,000 (HuH1 and HuH7) or 700 mm^3 (HLF) (Fig. 4D). The high metastatic capacity of PLC/PRL/5 cells, which contain a small population of $CD90^+$ cells, was also confirmed after SC injection into NOD/SCID mice (data not shown). $CD90^+$ cells could divide to generate both $CD90^+$ and $CD90^-$ cells, and $CD90^+$ cells showed a high capacity to invade and form spheroids with overexpression of *TWIST1* and *TWIST2*, which are known to activate EMT programs in HLF cells (Supporting Fig. 2A-D).

We next evaluated the tumorigenic/metastatic capacity of $CD45^-$ tumor cells using 12 fresh primary HCC specimens (P1-P12) that had been surgically resected (Table 2). We further evaluated the tumorigenicity of EpCAM/CD90 sorted cells obtained from xenografts derived from primary HCCs (Supporting Fig. 3A). Of these, we confirmed the tumorigenicity of cancer cells obtained from six primary HCCs after SC injection into NOD/SCID mice within 3 months after transplantation (Fig. 5A; Table 2; Supporting Fig. 3B). $EpCAM^+$ cells derived from four HCCs (P4, P7, P13, and P14) showed highly tumorigenic capacities, compared with $EpCAM^-$ cells. $CD90^+$ cells derived from two HCCs showed equal (P12) or more-tumorigenic capacities (P15), compared with $CD90^-$ cells. Tumorigenicity of $EpCAM^+$ cells was observed in three hepatitis C virus (HCV)-related HCCs and an hepatitis B virus (HBV)-related HCC, whereas tumorigenicity of $CD90^+$ cells was observed in two HBV-related HCCs (Tables 1 and 2).

Using unsorted cells, we compared the frequency of $EpCAM^+$ and $CD90^+$ cells in primary and xenograft tumors and found that $EpCAM^+$ cells remained, but $CD90^+$ cells disappeared, in secondary tumors derived from P4 or P7, whereas $EpCAM^+$ cells disappeared, but $CD90^+$ cells remained, in secondary tumors derived from P12 (Fig. 5B). Morphologically, tumorigenic $EpCAM^+$ cells showed an epithelial cell shape, whereas $CD90^+$ cells showed a mesenchymal VEC shape (Fig. 5C and Supporting Fig. 3C). FACS analysis indicated that P12 HCC cells showed abundant expression of vascular endothelial growth factor receptor (VEGFR) 1 and a vascular endothelial marker endoglin (CD105) (Fig. 5D). By contrast, P4 and P7 HCC cells did not express these vascular endothelial markers (data not shown). Lung metastasis was detected in NOD/SCID mice transplanted with P12 HCC cells, but not in mice transplanted with P4 and P7 HCC cells (Fig. 5E,F).

Taken together, these results suggest that the tumorigenic and metastatic capability of primary HCC may depend on the presence of distinct $EpCAM^+$ or $CD90^+$ CSCs. $EpCAM^+$ cells were associated with a high tumorigenic capacity with hepatic epithelial stem cell features, whereas $CD90^+$ cells were related to the metastatic propensity with VEC features.

Suppression of Lung Metastasis Mediated by $CD90^+$ CSCs by Imatinib Mesylate. We previously demonstrated that Wnt/β-catenin signaling inhibitors could successfully attenuate the tumorigenic capacity of $EpCAM^+$ CSCs in HCC.[8,10] To explore the potential molecular targets activated in $CD90^+$ CSCs, we investigated the expression of the known VEC markers, CD105, VEGFR1 (encoded by *FLT1*), and

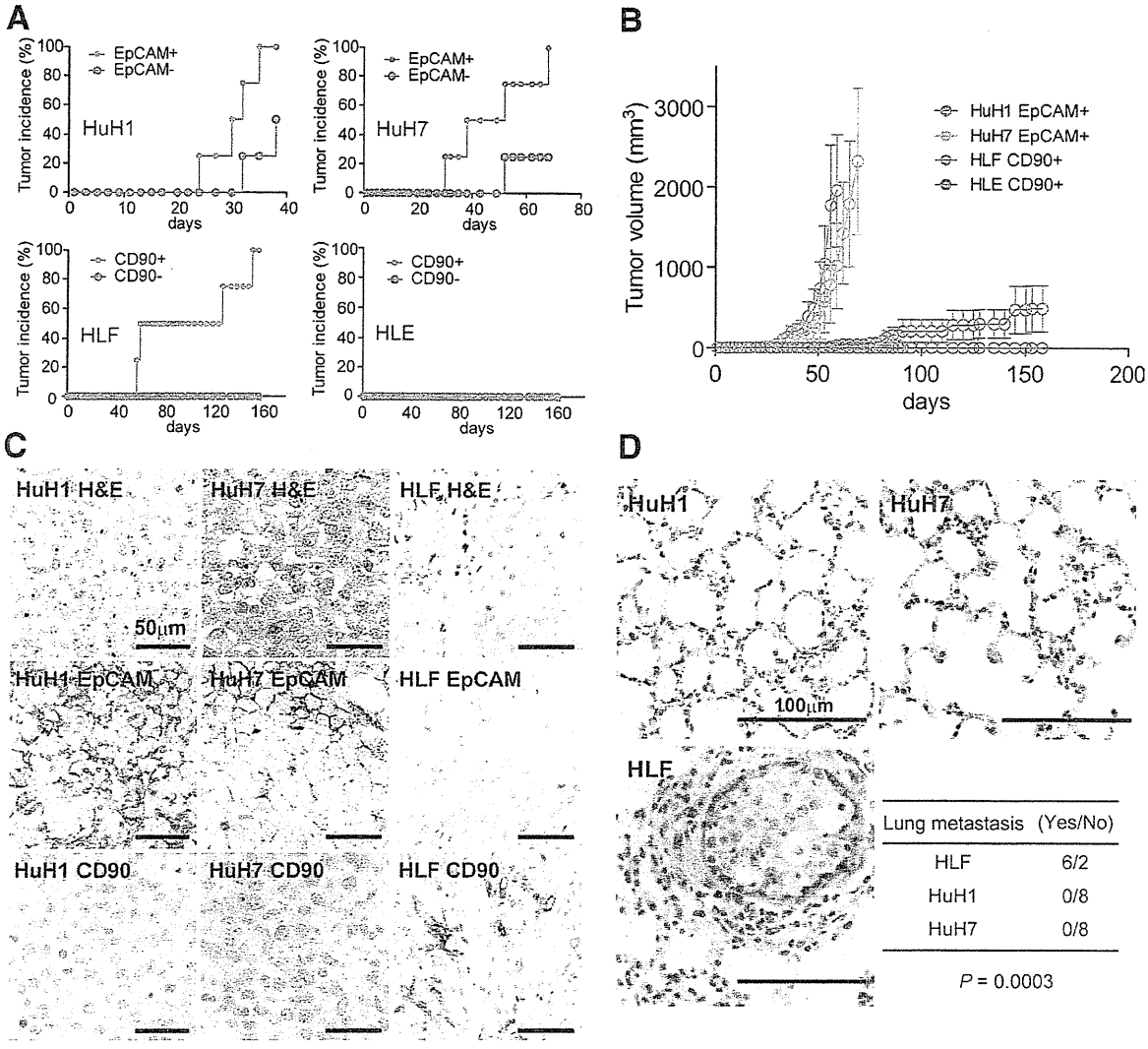

Fig. 4. Distinct tumorigenic/metastatic capacities of HCC cell lines defined by EpCAM and CD90. (A) Tumorigenicity of 1×10^5 cells sorted by anti-EpCAM (HuH1 and HuH7) or anti-CD90 (HLE and HLF) Abs. Data are generated from 8 mice/cell line. (B) Tumorigenic ability of $EpCAM^+$ and $CD90^+$ sorted cells in NOD/SCID mice. Aggressive tumor growth in the SC lesion was observed in $EpCAM^+$ HuH1 or HuH7 cells, compared with $CD90^+$ HLE or HLF cells. $EpCAM^+$ (1×10^5) or $CD90^+$ cells were injected. Tumor-volume curves are depicted as mean ± standard deviation of 4 mice/group. (C) Histological analysis of $EpCAM^+$ or $CD90^+$ cell-derived xenografts. Hematoxylin and eosin (H&E) staining of a SC tumor (upper panels) and IHC of the tumor with anti-EpCAM (middle panels) or anti-CD90 Abs (bottom panels) are shown (scale bar, 50 μm). (D) Metastasis was evaluated macroscopically and microscopically in the left and right lobes of the lung separately in each mouse (n = 4) (scale bar, 100 μm).

c-Kit (encoded by *KIT*), in cell lines and showed that they were abundantly expressed in $CD90^+$ cell lines, but not $EpCAM^+$ cell lines (Fig. 6A). No expression of VEGFR2 was detected in this set of cell lines, suggesting that molecular reagents specifically targeting VEGFR2 may have no effects on $CD90^+$ CSCs. CD44, a stem cell marker that functionally regulates redox status and is a potential target of $CD90^+$ CSCs, was also abundantly expressed in $CD90^+$ cell lines (Supporting Fig. 4A), consistent with previous data.[5,13] No significant difference was detected in the expression of the hematopoietic marker, CD34, or ABCG2 between $EpCAM^+$ and $CD90^+$ cell lines (Supporting Fig. 4A).

Among these molecular targets, we focused on the characterization of c-Kit because the c-Kit tyrosine kinase inhibitor, imatinib mesylate, is readily available, is widely used for the treatment of gastrointestinal stromal tumor with activation of c-Kit, and may have potential antitumor activity against a subset of HCC.[14] We explored the effect of imatinib mesylate on HCC cell lines and found that treatment with 10

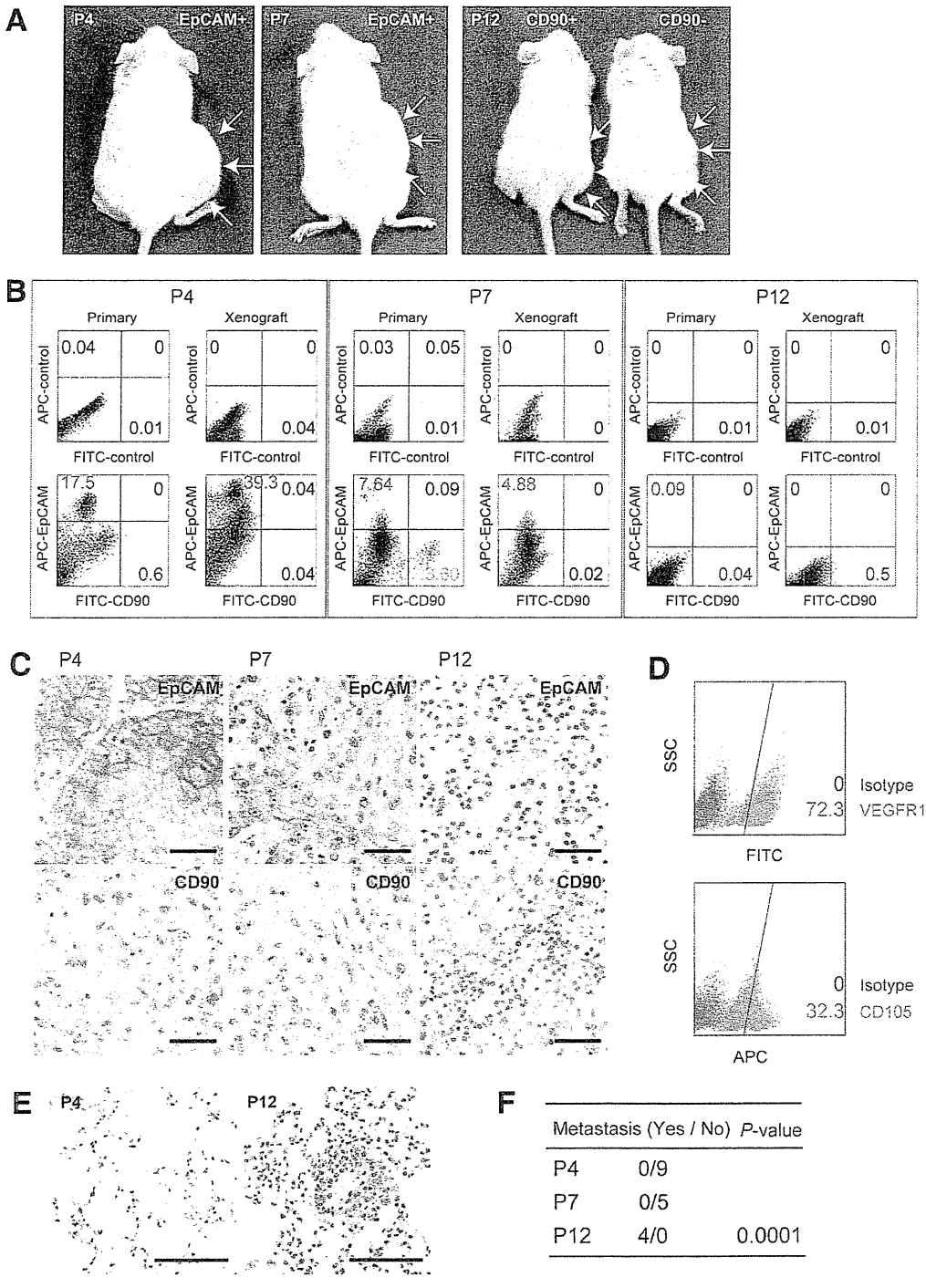

Fig. 5. Tumorigenic/metastatic capacities of EpCAM$^+$ and CD90$^+$ cells in primary HCC. (A) Representative NOD/SCID mice with SC tumors (white arrows) from EpCAM$^+$ P4 or P7 cells (left and middle panels) and CD90$^+$ or CD90$^-$ P12 cells (right panel). (B) FACS analysis of CD90 and EpCAM staining in primary HCCs and the corresponding secondary tumors developed in NOD/SCID mice. Unsorted cells (1×10^6 cells in P4 and P7 or 1×10^5 cells in P12) were SC injected to evaluate the frequency of each marker-positive cell in primary and secondary tumors. (C) IHC analysis of EpCAM and CD90 in primary HCCs P4, P7, and P12 (scale bar, 50 μm). (D) FACS analysis of VEGFR1 (Alexa488) and CD105 (APC) in primary HCC P12. (E) Hematoxylin and eosin staining of lung tissues in P4 and P12 (scale bar, 200 μm). (F) Frequency of lung metastasis in NOD/SCID mice SC transplanted using unsorted primary HCC cells.